Stockwork GeoConsulting Ltd.

UNIVERSITATEA BABEȘ-BOLYAI
BABEȘ-BOLYAI TUDOMÁNYEGYETEM
BABEȘ-BOLYAI UNIVERSITÄT
BABEȘ-BOLYAI UNIVERSITY
TRADITIO ET EXCELLENTIA

Geochemical vectors in mineral exploration: integration, interpretation and modelling of high-precision multielement and hyperspectral datasets

István MÁRTON, PhD

Lecture D2U1 – part II.

DIM ESEE

DIM ESEE 2: IMPLEMENTING INNOVATIONS

Innovation in Exploration

Dubrovnik, Croatia / hybrid mode - October 20th – 22nd, 2021

Content

Recent developments in exploration geochemistry and better instrumentation of industrial geochemical laboratories provide large and high-precision partial digestion multi-element datasets for mineral exploration projects. Additionally, the expansion of portable and benchtop XRF, SWIR and XRD devices deliver fast and reliable characterization of mineralogy and geochemistry of drill core, soil and rock samples. Furthermore, tripod- and UAV-based hyperspectral scanning and satellite-based remote sensing deliver high-resolution alteration and lithology maps for pits, underground galleries and surface outcrops. These exploration geochemical datasets provide critical information about ore genetic and mineralization controlling aspects, about alteration footprint and optimal drill-spacing, about vectors to fertile host rocks and economic mineralization and on perspectives of geometallurgical domaining at any mineral exploration project.
This second part of the lesson will assess various tools for 2D and 3D integration, geostatistical methodologies and interpretation of high-precision multielement and spectral datasets and the review of various geochemical vectors used in mineral exploration:

1. Introduction to magmatic-hydrothermal systems

2. Geochemical vectors in magmatic-hydrothermal systems

3. Vectoring tools, geostatistical methodologies and interpretation of exploration geochemical data on the example of Chelopech Cu-Au(Ag-Pb-Zn-Mo) mineralization

Introduction to magmatic-hydrothermal acid-sulphate systems

Introduction to magmatic-hydrothermal acid-sulphate systems

Crustal scale phenomenon of magmatic-hydrothermal systems

Acid-sulphate alteration environment

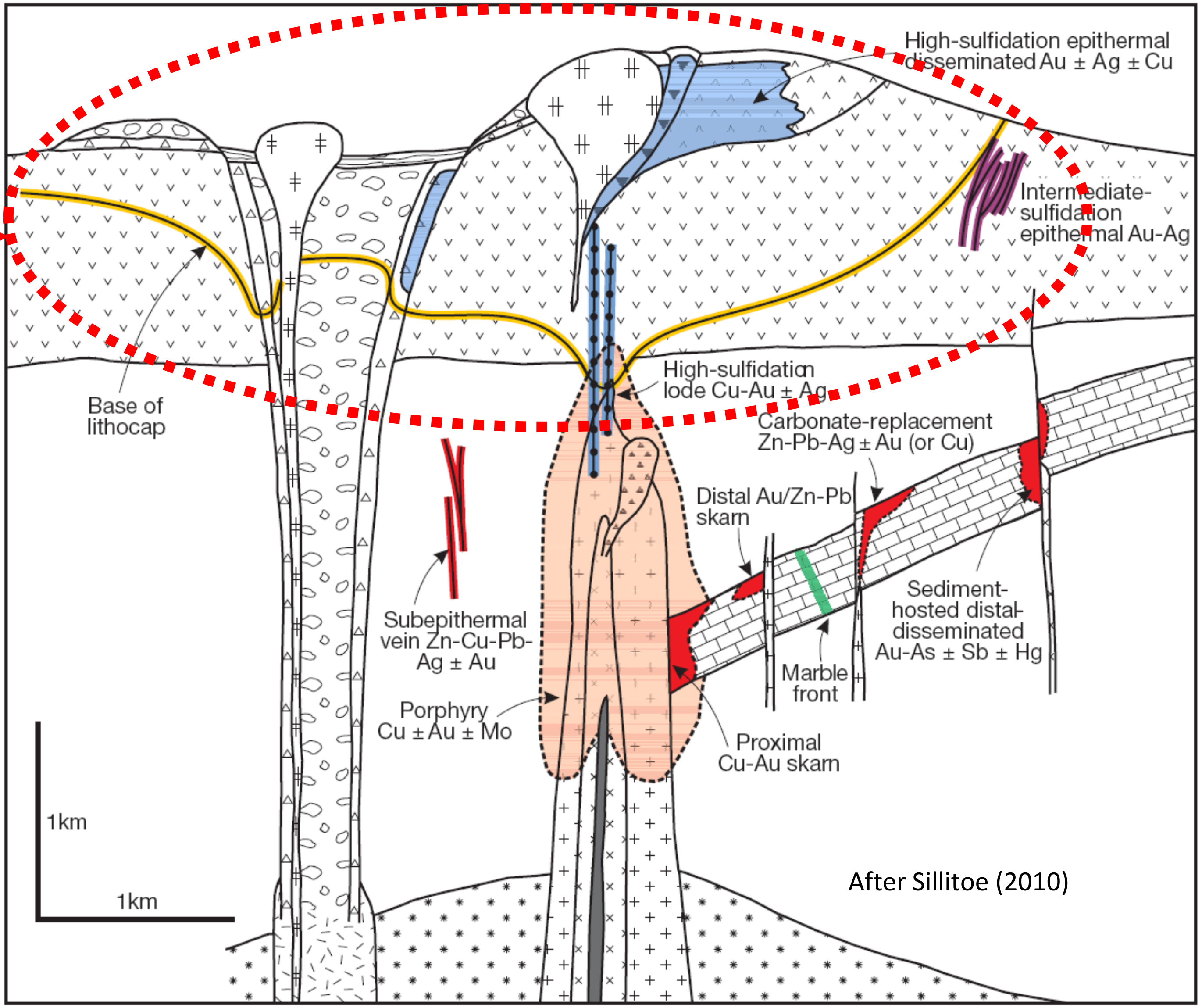

- Input of magma into crust and construction of upper crustal magma chamber
- Exsolution of hydrothermal fluid and buoyant rise into porphyry and epithermal environment

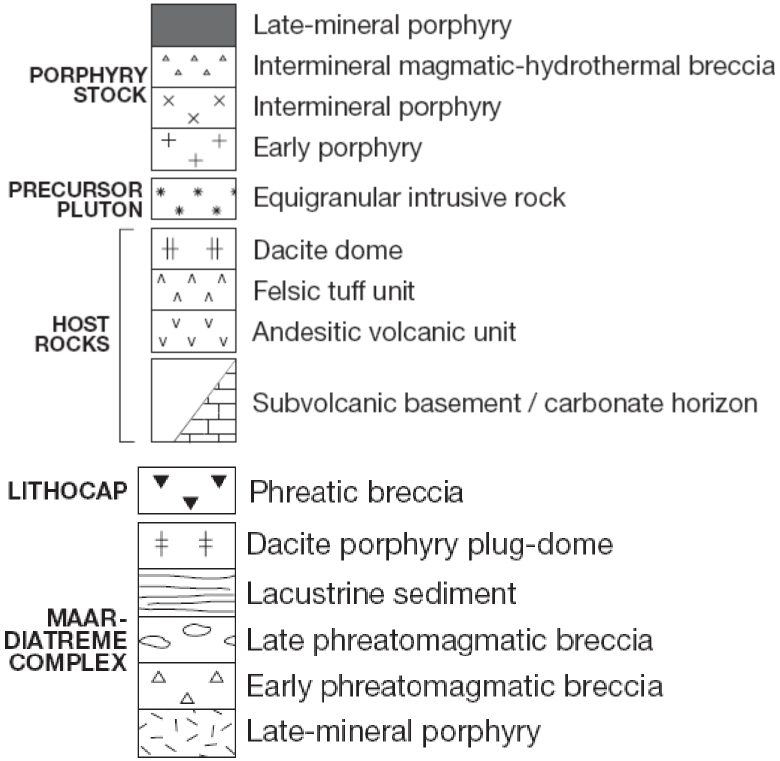

Introduction to magmatic-hydrothermal acid-sulphate systems

Fluids involved in magmatic-hydrothermal systems

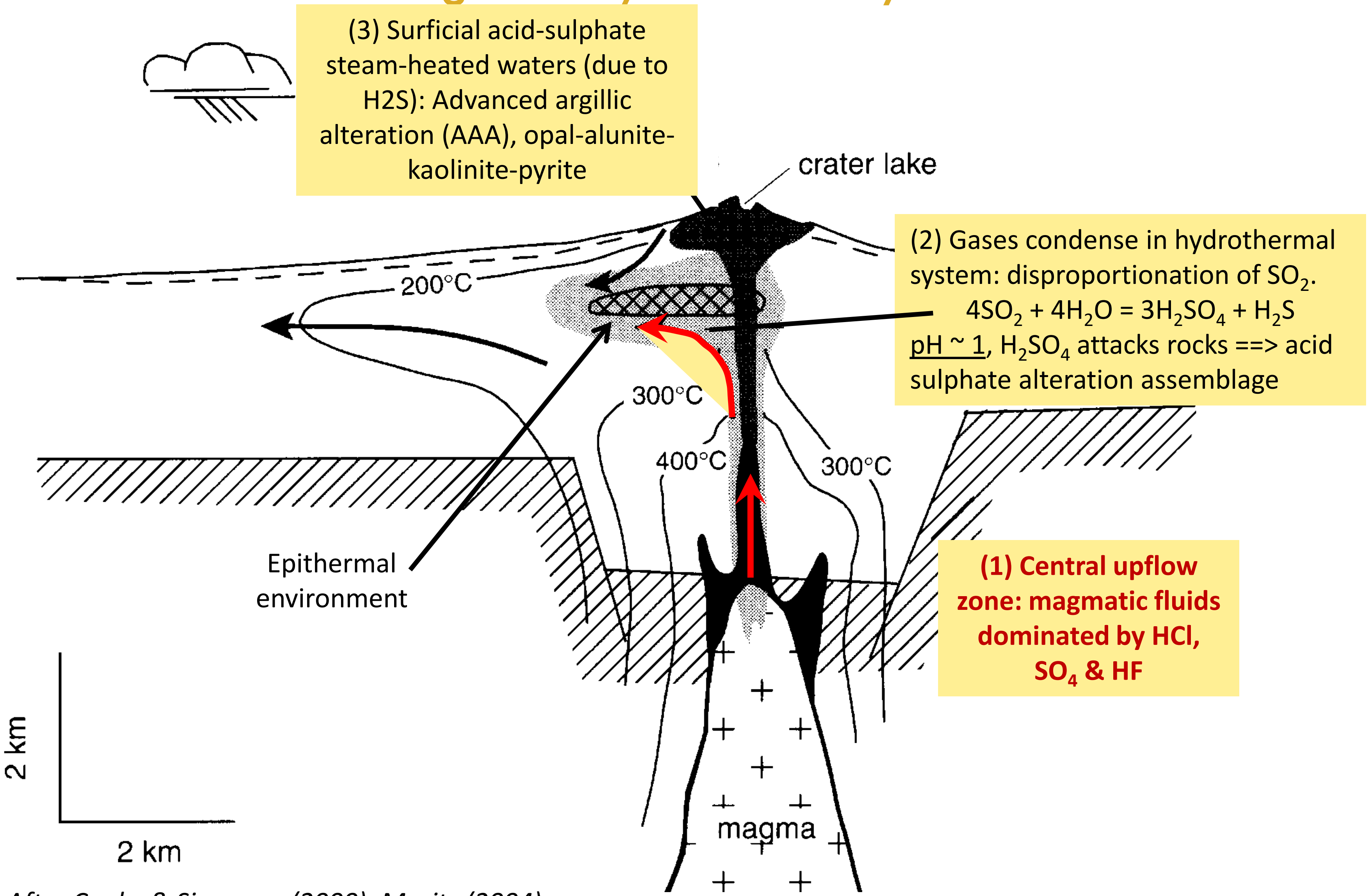

After Cooke & Simmons (2000), Moritz (2004)

Fluid-dominated alteration, hydrolysis reactions and fluid-rock interactions neutralize acidity

==>

Acid-sulphate or Advanced argillic alteration (AAA)

Incl. alunite-pyrophyllite-dickite-kaolinite-vuggy quartz-anhydrite-diaspore-topaz-zunyite-APS minerals (alumino-phosphate-sulfate)

Introduction to magmatic-hydrothermal acid-sulphate systems

Fluids involved in magmatic-hydrothermal systems

Decreasing T increases dissociation of salts & acids (K+ and H+ increase relative to KCl & HCl)
→ dissociation of acids (HSO_4^-, HCl, H_2CO_3) leads to real acidity increase and sulfide deposition

Important alteration processes:

- Hydrolytic (acidic), $H^+ = K^+$
- Alkali exchange, $Na^+ = K^+$
- Precipitation/dissolution, quartz
- Oxidation/reduction (S_2, O_2)

Greater fluid-rock interaction
→ neutralizes acidity (H)

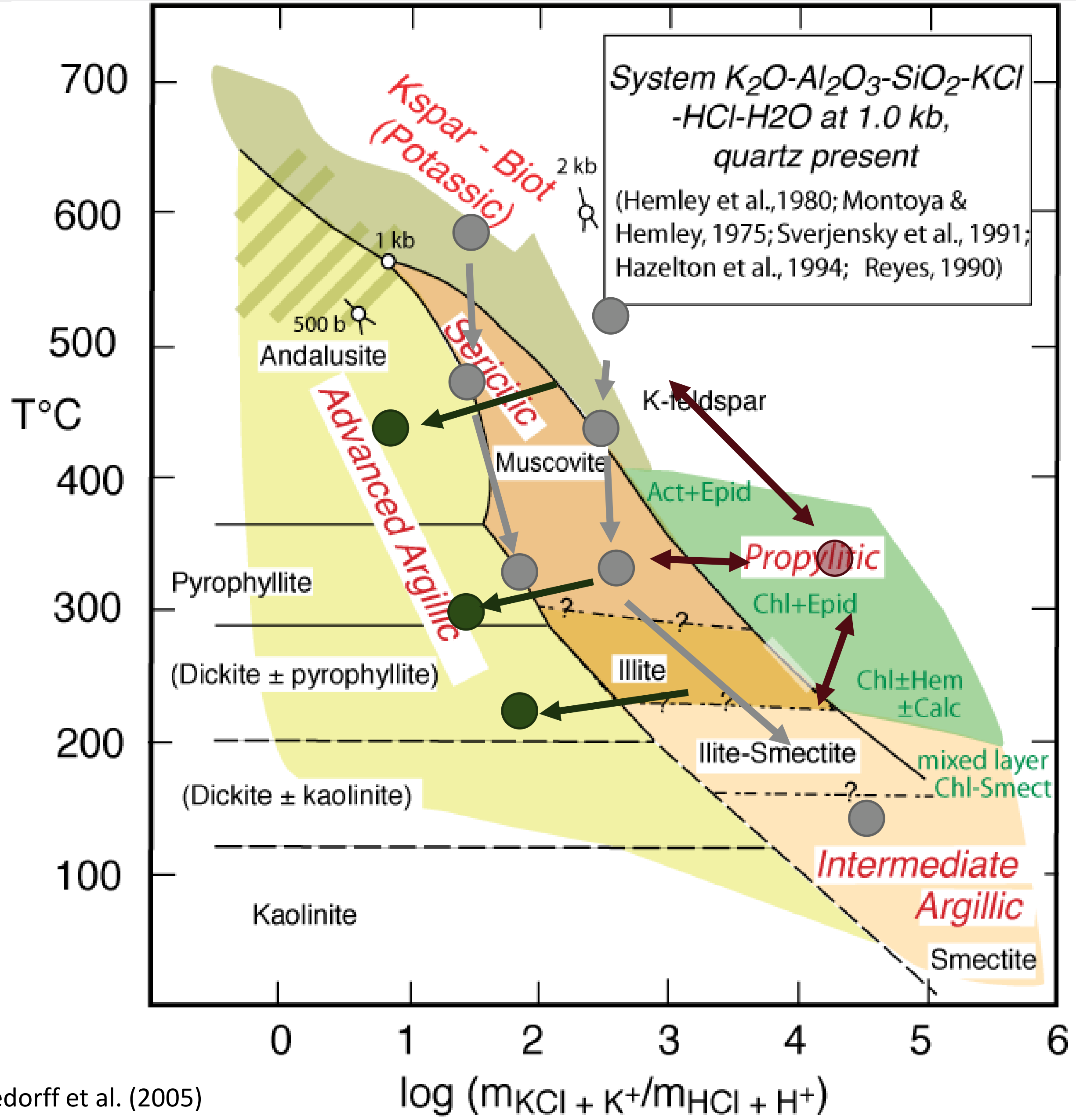

After Seedorff et al. (2005)

Introduction to magmatic-hydrothermal acid-sulphate systems

Depth-temperature controls on hypogene acid-sulphate systems (Hedenquist et al., 2000)

Depth (m)	Paleosurface–water table	0–150 m	150–300 m	300–500 m	500–1,000 (1,500) m
Temp. (°C)	100–120	100–200	200–230	230–260	260–300+
Advanced argillic alteration	Steam-heated kaolinite-alunite blanket; residual opal, cristobalite	Quartz-alunite halo to silicic core	Wide quartz-alunite halo, depending on host	Flaring upward, quartz-alunite; pyrophyllite, diaspore	Narrow zones, pyrophyllite, sericite
Silicic alteration	Chalcedony horizon at water table	Chalcedony veins, residual silica, vuggy quartz, silicification	Residual silica, vuggy quartz, silicification	Residual silica, vuggy quartz, silicification	Quartz D-type porphyry veins
Argillic alteration	Kaolinite-smectite	Smectite-interlayered illite/smectite	Transitional to sericitic	On margins	On margins
Sericitic alteration	None	None	None	Illite-sericite, to sericite-pyrophyllite	Sericite-pyrophyllite to 2M mica
T-sensitive or indicative	Opal	Chalcedony	Loss of interlayered clays	Pyrophyllite	Biotite
Sulfides	Pyrite-marcasite at base	Pyrite-marcasite at base, transitional to Cu-As-Sb sulfides/sulfosalts	Enargite-luzonite with later Au+ tennantite-tetrahedrite-chalcopyrite	Enargite-luzonite with later Au+ tennantite-tetrahedrite-chalcopyrite	Enargite, bornite, digenite, chalcocite, covellite

Introduction to magmatic-hydrothermal acid-sulphate systems

Typical alteration and mineralization paragenesis of acid-sulphate (high-sulphidation) systems

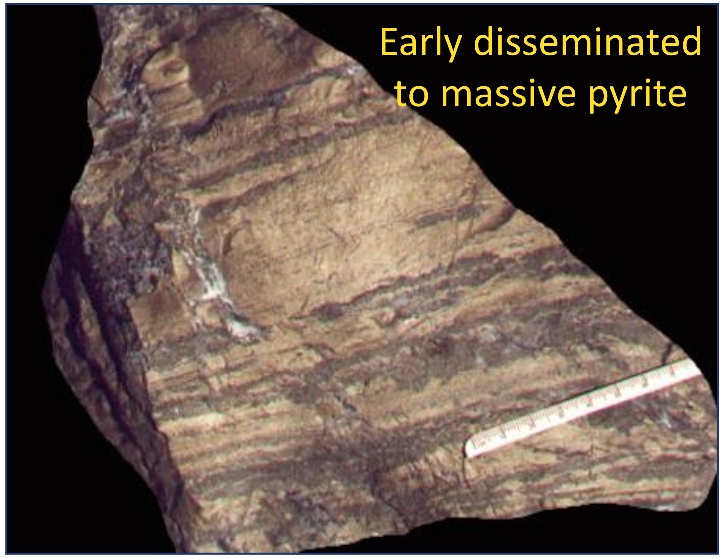

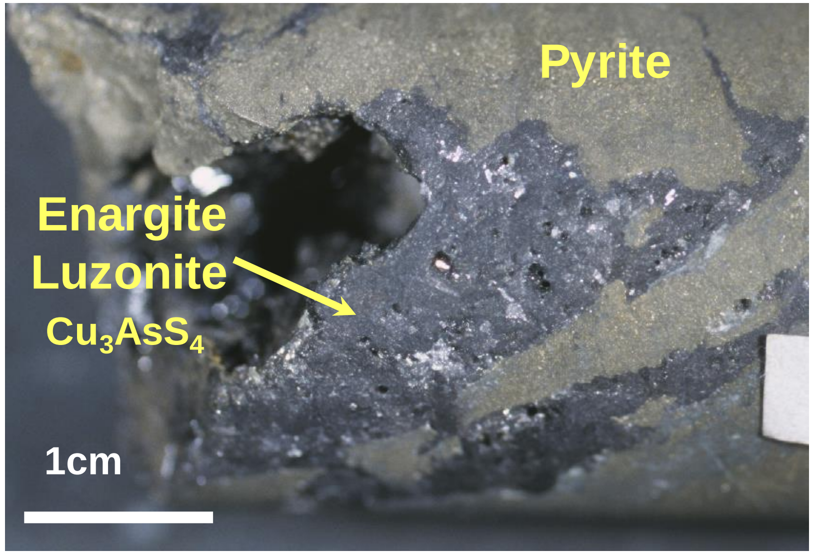

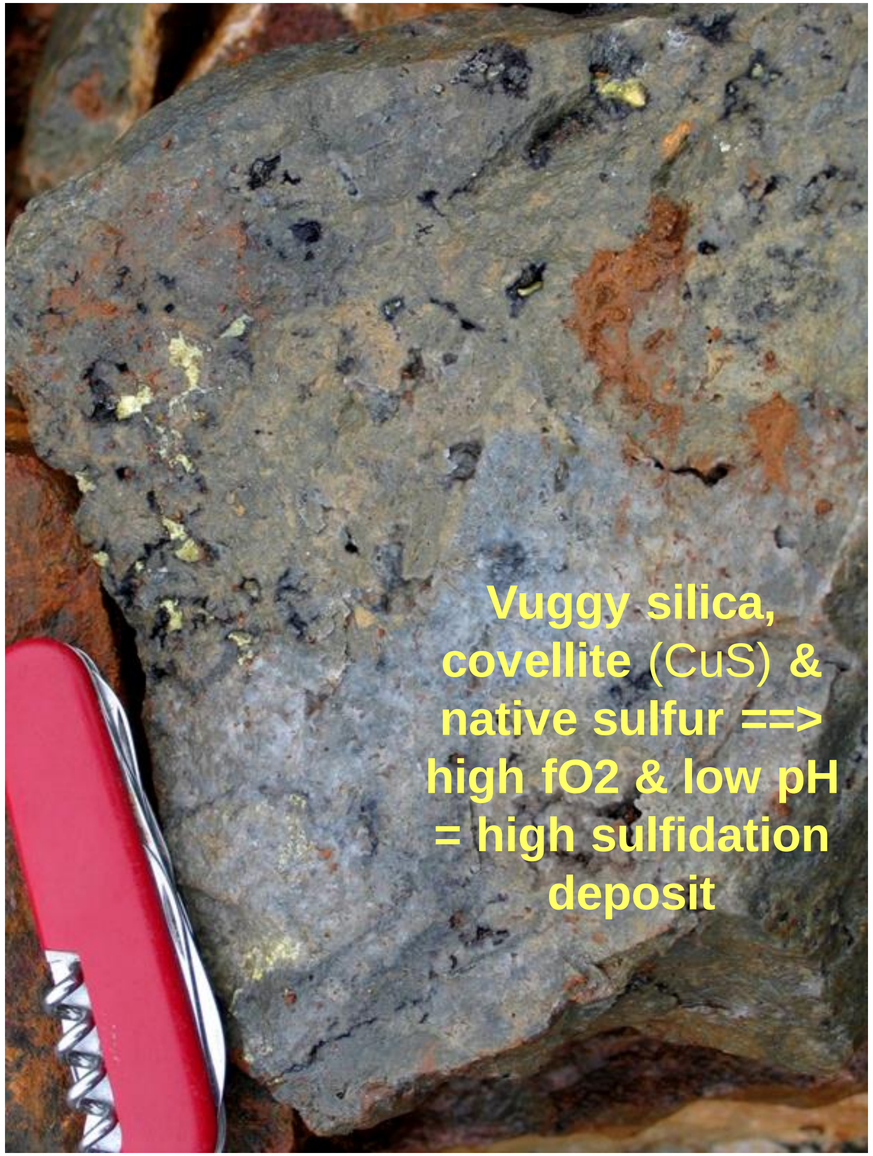

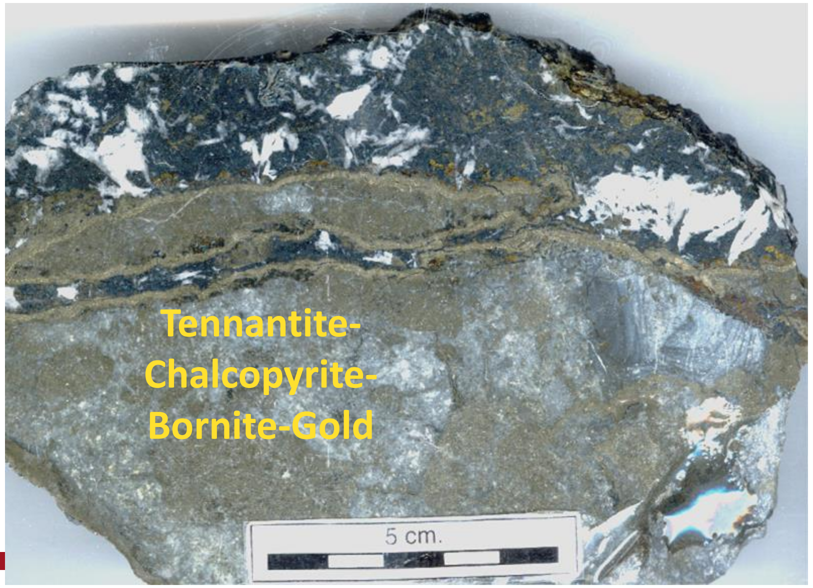

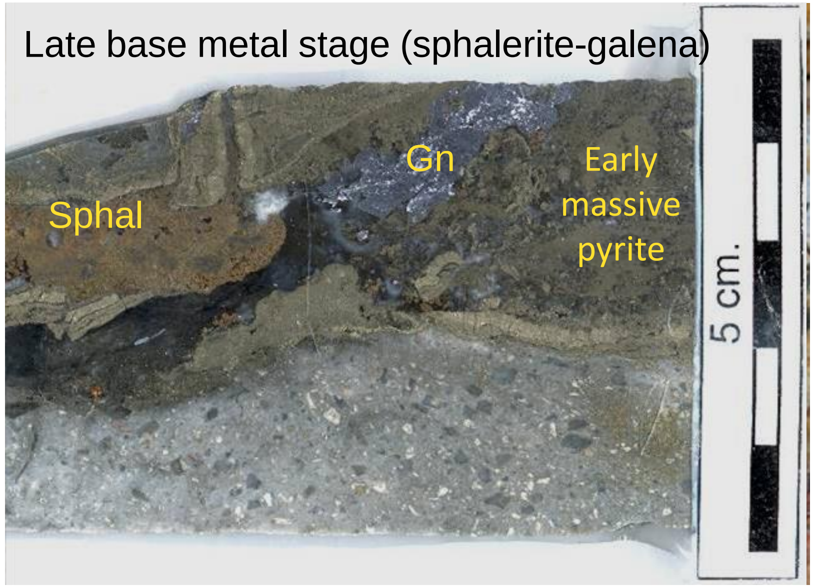

Introduction to magmatic-hydrothermal acid-sulphate systems

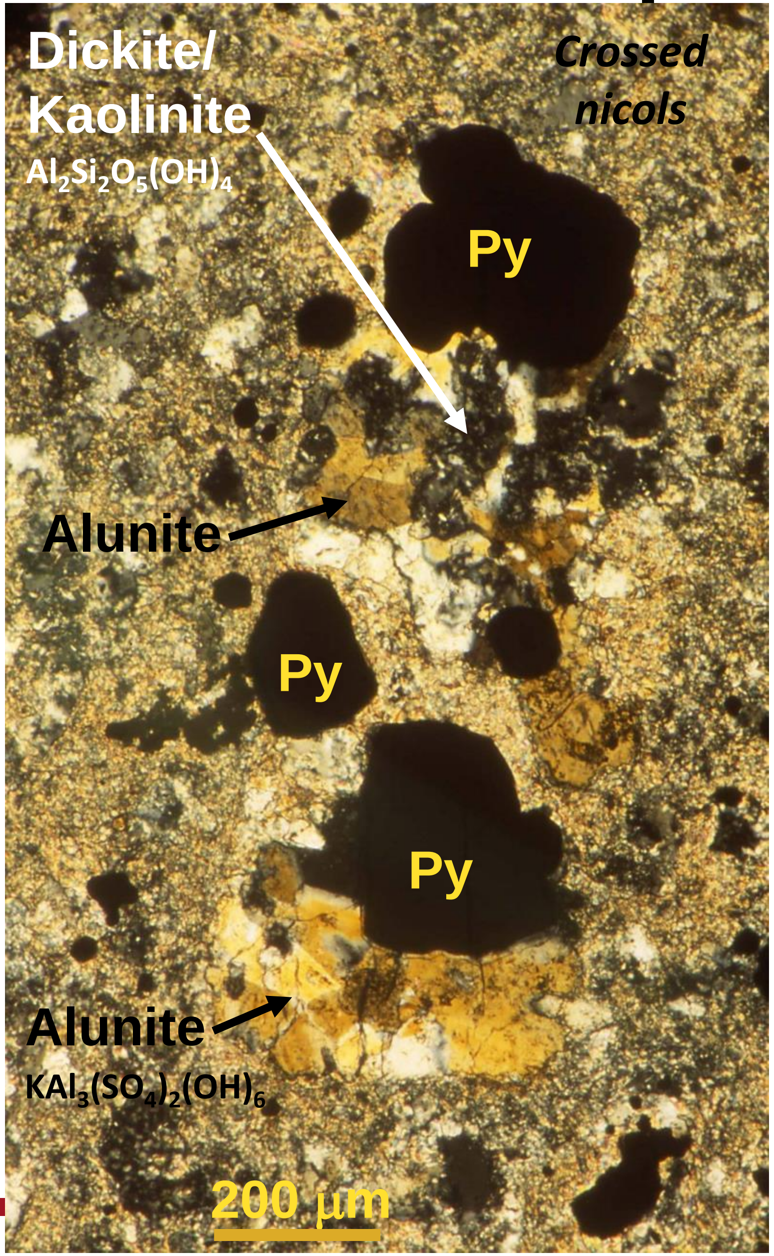

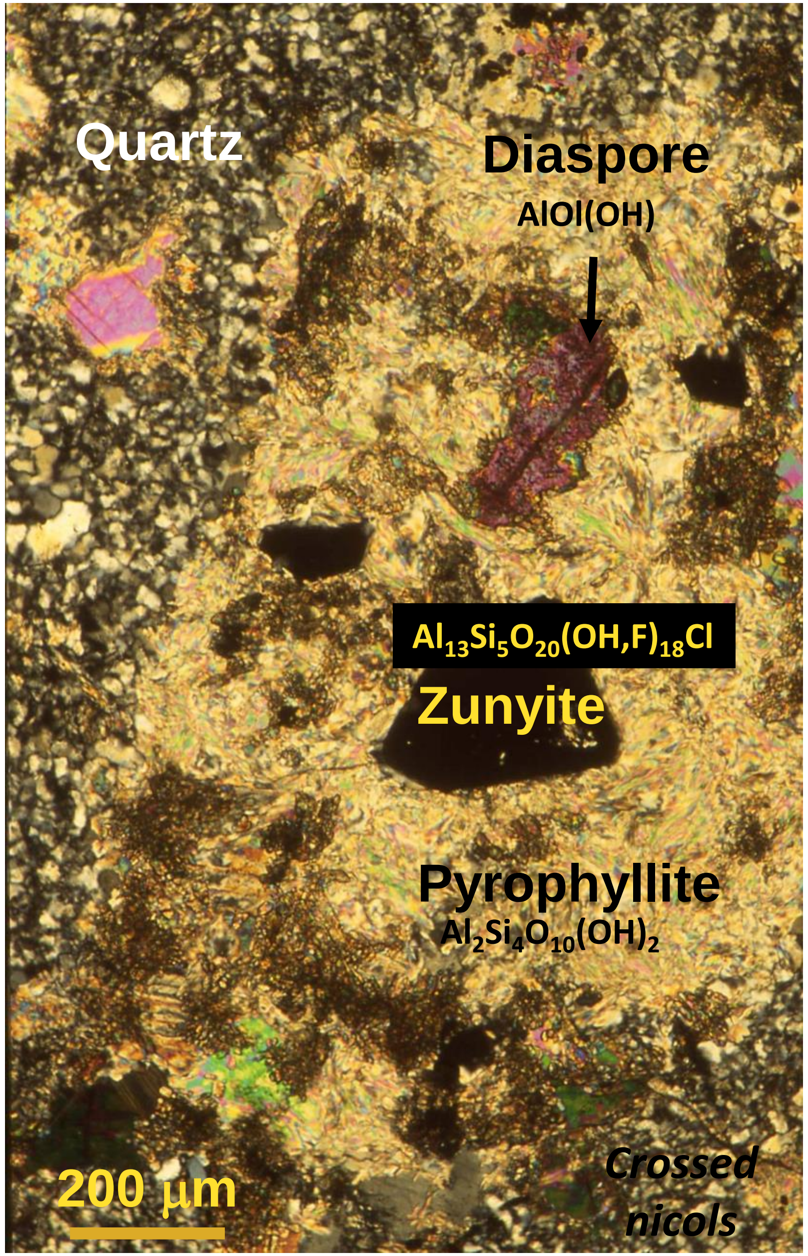

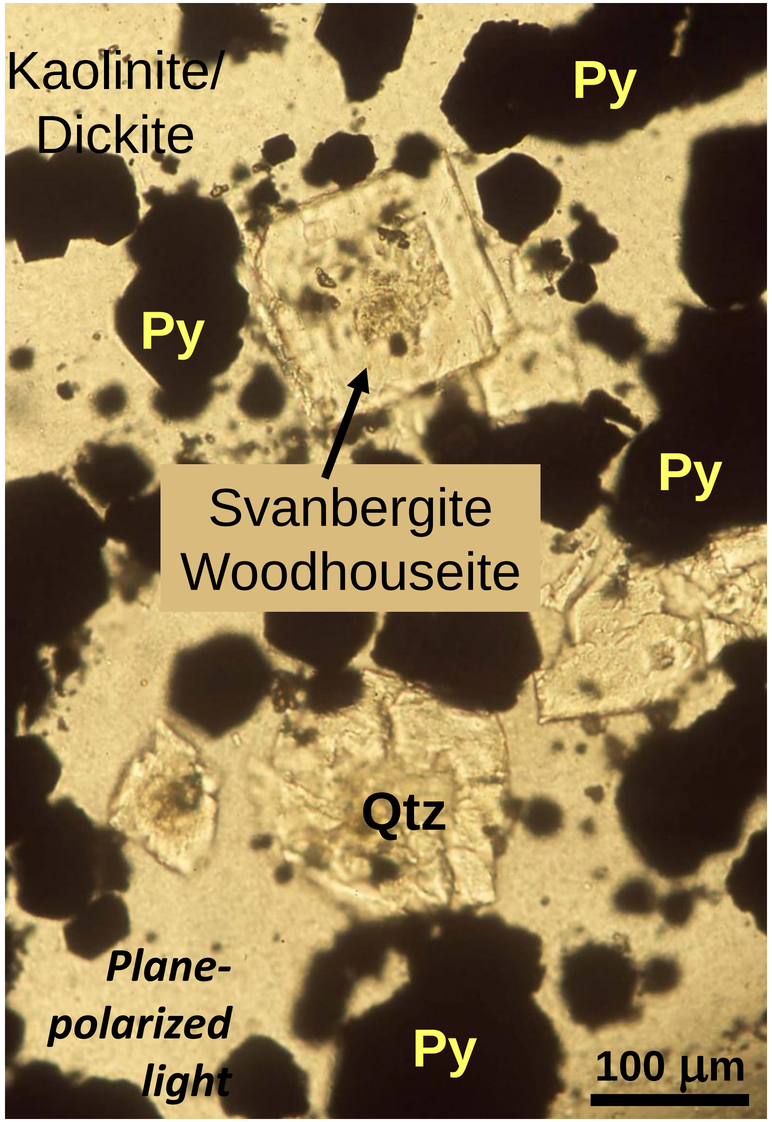

From Moritz & Chambefort (2005)

Introduction to magmatic-hydrothermal acid-sulphate systems

Alumino-phosphate minerals (APS - Alunite Supergroup) acid-sulphate systems

White alunite & kaolinite in a steam-heated zone affecting rhyolite tuff above the water table (Király-hegy, Hungary)

Alunite series	
Alunite	$KAl_3(SO_4)_2(OH)_6$
Natroalunite	$NaAl_3(SO_4)_2(OH)_6$
Natrojarosite	$NaFe_3(SO_4)_2(OH)_6$
Jarosite	$KFe_3(SO_4)_2(OH)_6$
Ammoniumjarosite	$(NH_4)Fe_3(SO_4)_2(OH)_6$
Hydronium alunite	$(H_3O)Al_3(SO_4)_2(OH)_6$
Minamiite	$Ca_{0.5}Al_3(SO_4)_2(OH)_6$
Woodhouseite series	
Woodhouseite	$CaAl_3(PO_4/SO_4)(OH)_6$
Svanbergite	$SrAl_3(PO_4/SO_4)(OH)_6$
Hinsdalite	$PbAl_3(PO_4/SO_4)(OH)_6$
Corkite	$PbFe(PO_4/SO_4)(OH)_6$
Kemmlitzite	$SrAl_3(AsO_4/SO_4)(OH)_6$
Crandallite series	
Crandallite	$CaHAl(PO_4)_2(OH)_6$
Goyazite	$SrHAl_3(PO_4)_2(OH)_6$
Gorceixite	$BaHAl_3(PO_4)_2(OH)_6$
Plumbogummite	$PbHAl_3(PO_4)_2(OH)_6$
Florencite	$(REE)Al_3(PO_4)_2(OH)_6$
Arsenocrandallite	$CaHAl_3(AsO_4)_2(OH)_6$
Philipsbornite	$PbHAl_3(AsO_4)_2(OH)_6$
Dussertite	$BaHFe_3(AsO_4)_2(OH)_6$
Segnitite	$PbHFe_3(AsO_4)_2(OH)_6$
Wardite series	
Wardite	$NaAl_3(PO_4)_2(OH)_4 \cdot 2H_2O$
Millisite	$(Na, Ca)Al_3(PO_4)_2(OH, O)_4 \cdot 2H_2O$

Introduction to magmatic-hydrothermal acid-sulphate systems

Geochemical vectoring in magmatic-hydrothermal systems (Halley et al., 2015)

A) Hydrothermal alteration assemblages

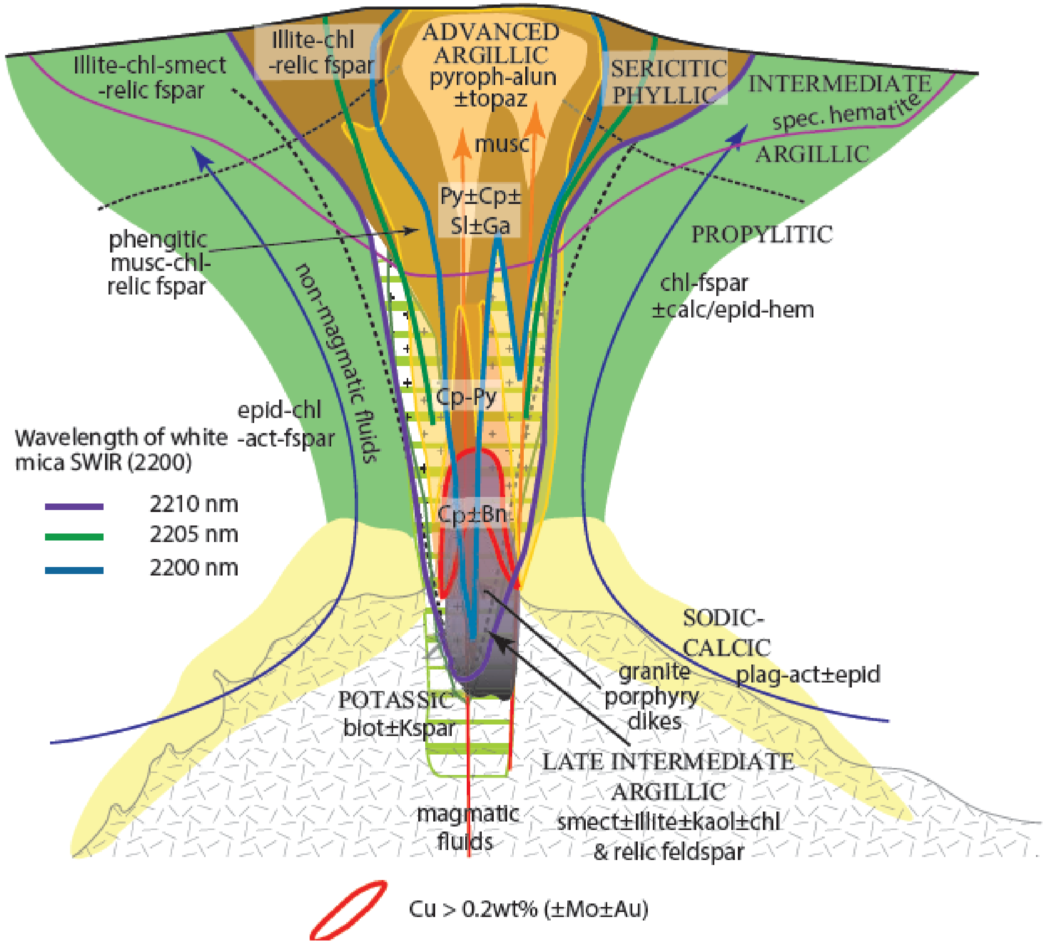

B) Vertical distribution of elements

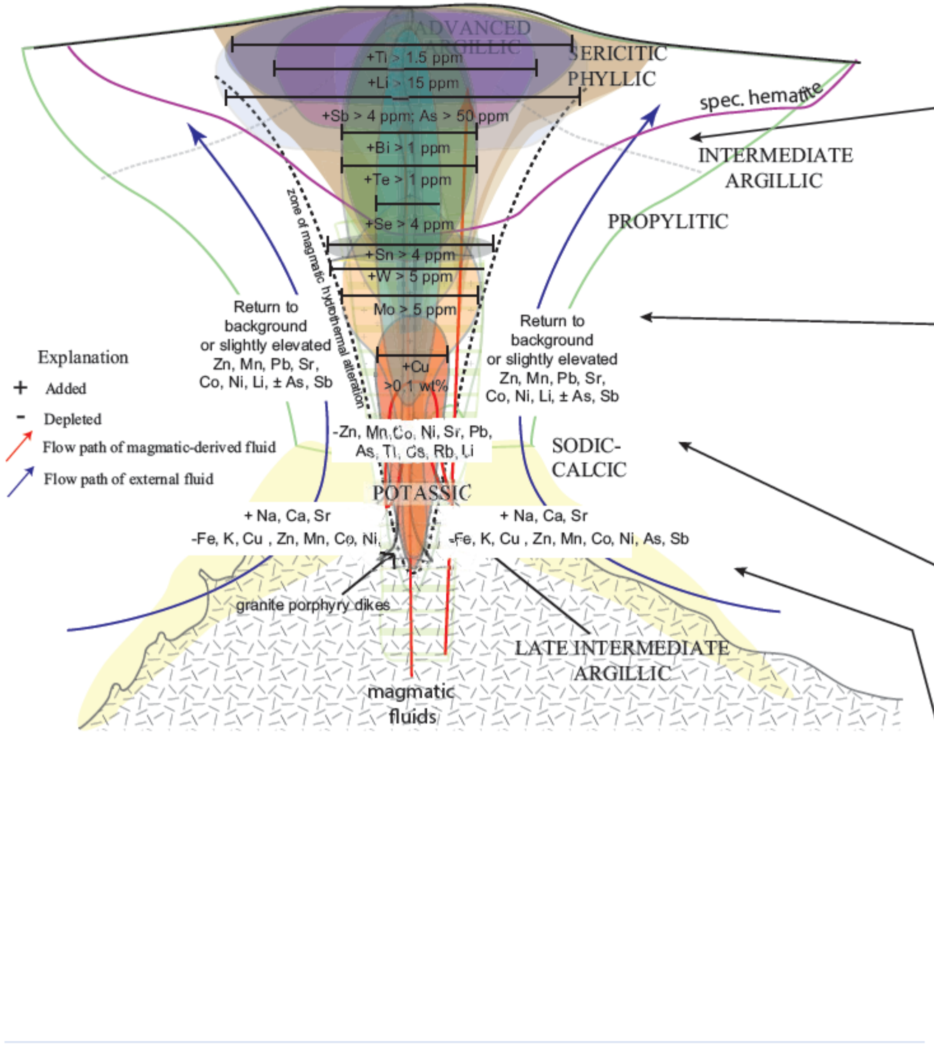

C) Lateral distribution of elements

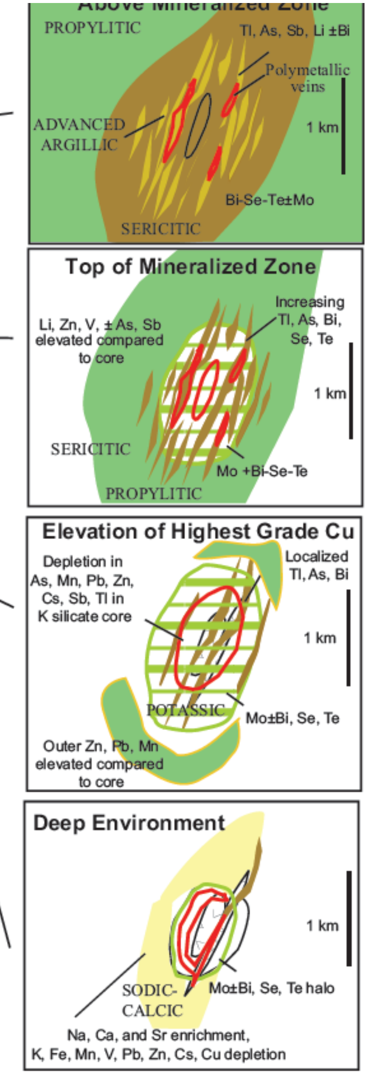

Case study I: Chelopech Au-Cu deposit, Bulgaria

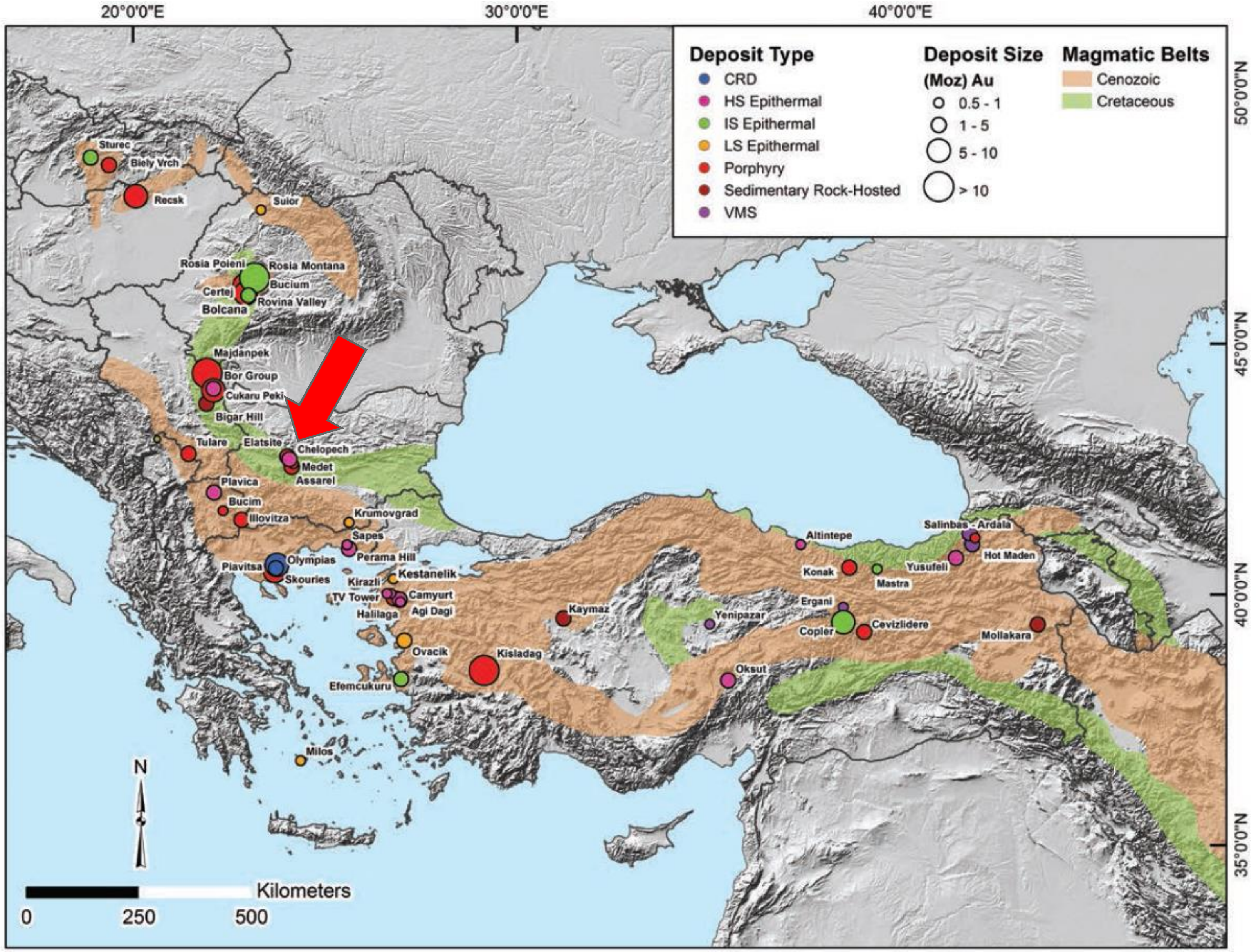

Baker (2019):
Location and styles of Au deposits (>0.5 Moz Au) related to Cretaceous and Cenozoic magmatism in the Western Tethyan magmatic belt.

Abbreviations: CRD = carbonate replacement deposit, HS = high sulfidation, IS = intermediate sulfidation, LS = low sulfidation, VMS = volcanogenic massive sulphide.

Chelopech Cu-Au deposit (Bulgaria)

Late Cretaceous magmatism and metal endowment of Panagyurishte district

- NE trending magmatism
- Younging from north to south (92 Ma – 78 Ma)

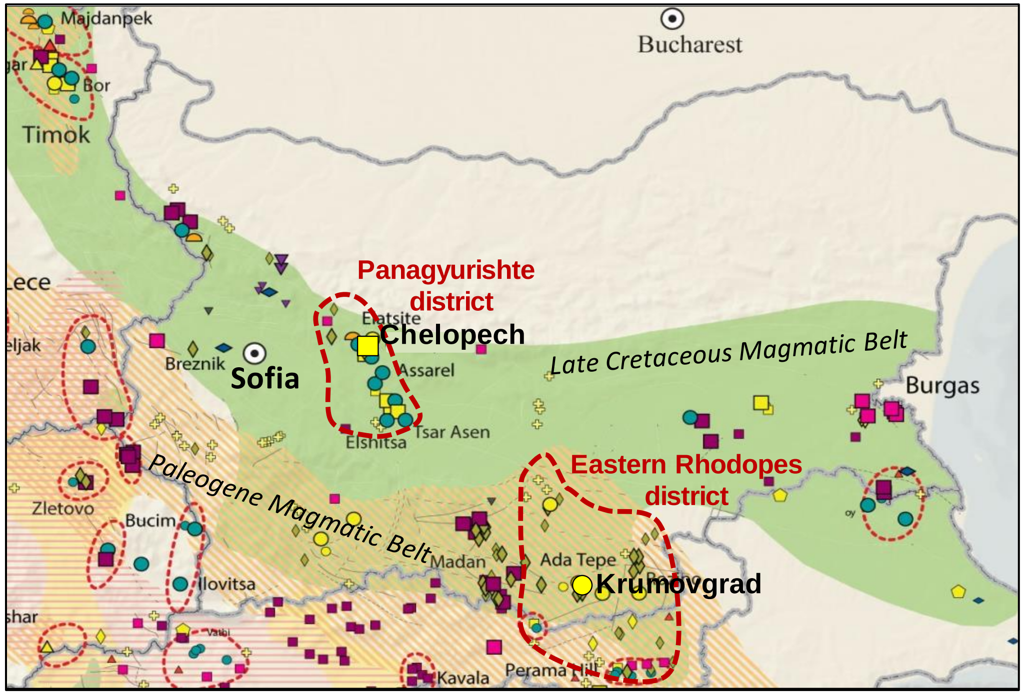

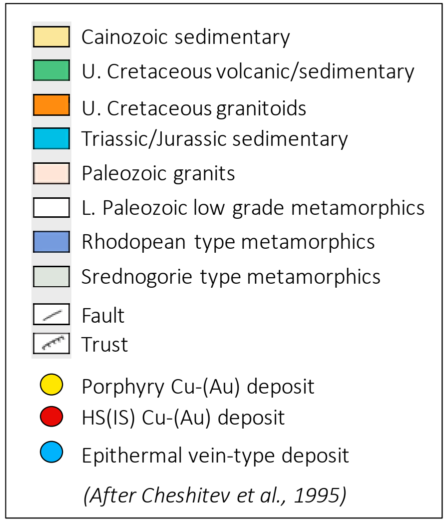

Data summarized in Von Quadt, Moritz, Peytcheva & Heinrich (2005)

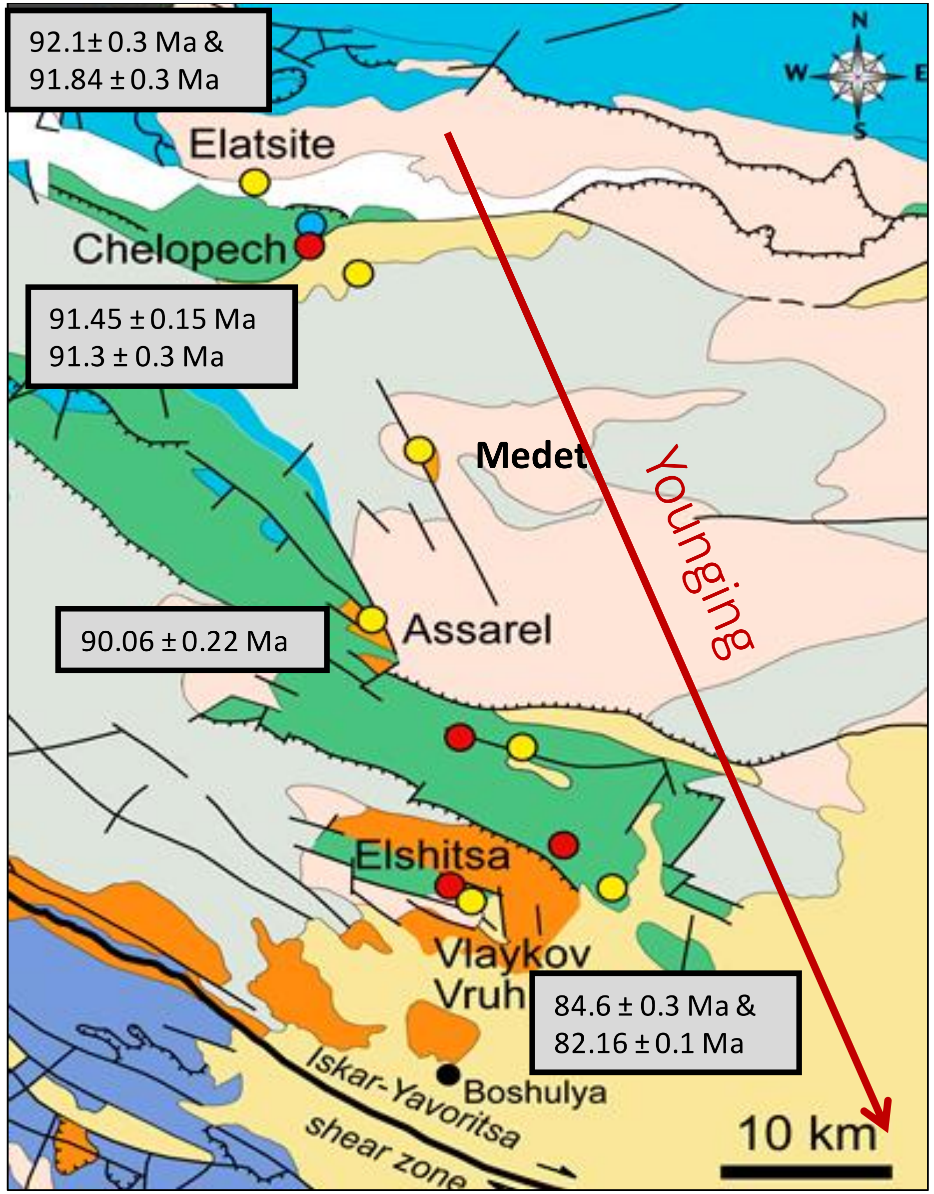

Chelopech Cu-Au deposit (Bulgaria)

Chelopech Cu-Au Mine: Solid Performer Focused on Optimization

- The deposit, having a considerable mining history since 1954, is operated as an underground mine by Dundee Precious Metals with an **annual production rate of 179,600 ounces of gold and 33.4 million pounds of copper (2.2 Mt ore processed) as per 2020**.
- Effective as of 31st December 2020, the Mine has a **Proven and Probable Mineral Reserve of 18.6Mt at 0.84% Cu, 2.89g/t Au and 7.73g/t Ag** and has a remaining Mineral Resource (exclusive of Mineral Reserves) of 17.4Mt (M+I) at an average grade of 0.82% Cu, 2.63g/t Au and 8.71g/t Ag.
- The reserves currently support an optimized mine life that extends to 2029.

TSX: DPM C$8.81 05/28/2021 4:00 PM Gold: US$1,906.88

About Us ▼ Ethics & Governance ▼ Media Releases

https://www.dundeeprecious.com/

Business Model & Strategy | Investors ▼ | Operating Regions ▼

Operating Regions
Current Operations
Chelopech, Bulgaria

Overview

Chelopech Proven and Probable Mineral Reserve Estimate (As at December 31, 2020)							
Classification	Tonnes	Gold		Silver		Copper	
	(Mt)	Grade (g/t)	K oz.	Grade (g/t)	K oz.	Grade (%)	Mlbs.
Proven	7.8	2.71	681	7.23	1,818	0.84	145.5
Probable	10.8	3.03	1,046	8.09	2,797	0.84	198.9
Total	18.6	2.89	1,727	7.73	4,615	0.84	344.4

- *Mineral Reserves are based on a cut-off value of $10 per tone profit margin (around 3 g/t AuEq).*
- *Long-term metal price assumed for the evaluation of Mineral Reserves and Mineral Resources are $1,400 per ounce for gold, $17.50 per ounce for silver, and $2.75 per pound for copper.*

Chelopech Cu-Au deposit (Bulgaria)

Chelopech Cu-Au Mine: ore bodies

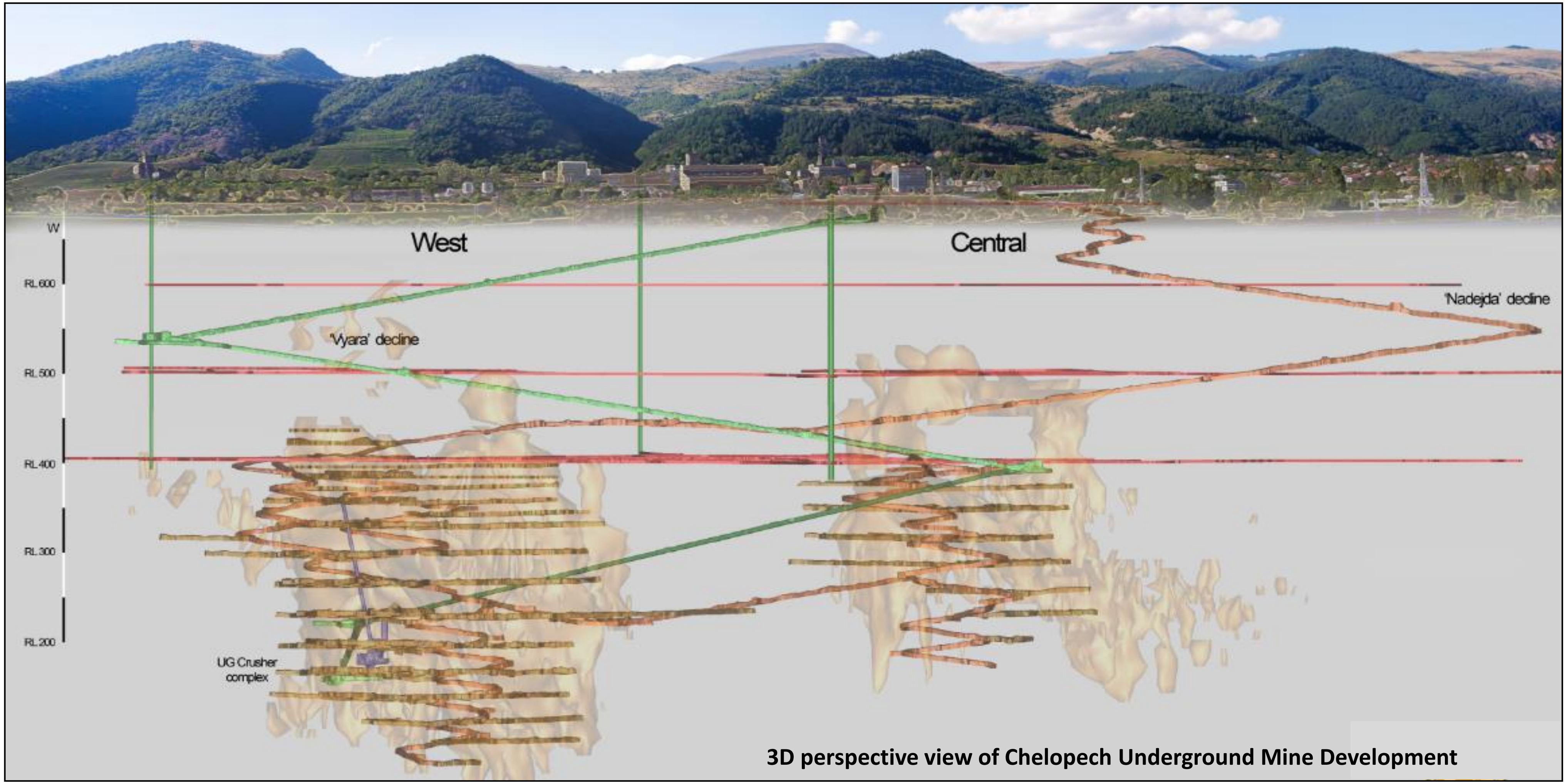

3D perspective view of Chelopech Underground Mine Development

- The ore bodies vary from 150-300 meters in length, are 30-120 meters thick and can extend at least 350 meters down plunge.
- The main ore bodies are spatially grouped into two mining areas, with semi-circular distribution and controlled by favorable breccia and host rock contact zones and structure intersections within the breccias.

Chelopech Cu-Au deposit (Bulgaria)

Chelopech Cu-Au Mine: mineralization

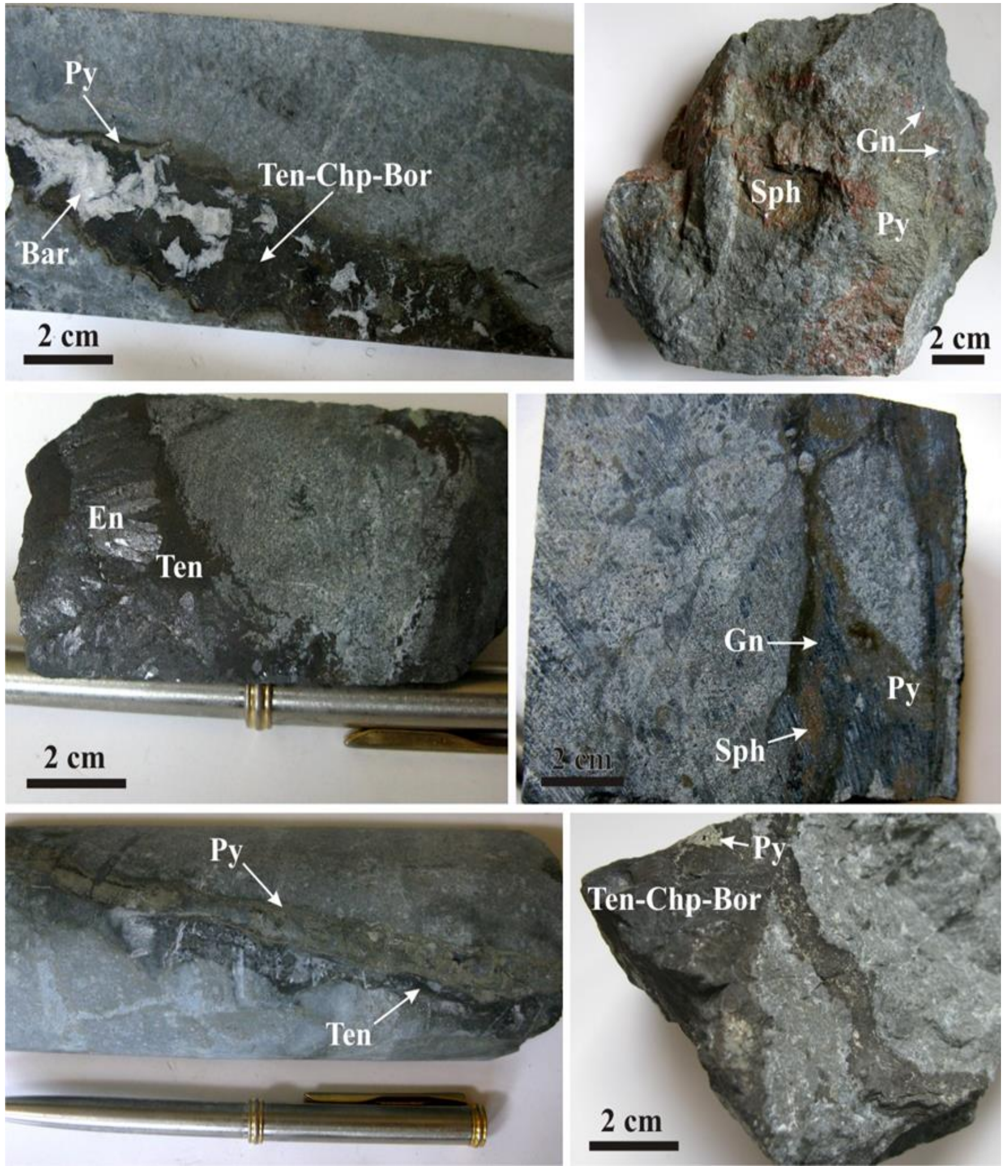

Ore Mineralization

Stockwork, vein and disseminated type of ore are most common among the different types breccia and among intrusive bodies.

Ore Minerals

Py, Tn, En-Luz, Au, Cpy & Bn with late stage Sp/Ga

Orebodies Morphology

Columnar pipe like bodies that typically plunge steeply towards the S & SE.

Alteration

Advanced argillic zone with “vuggy” silica and massive silica localities with quartz, dickite, kaolinite, pyrite, pyrophillite and alunite

Sericitic zone, characterized with quartz, sericite, illite, kaolinite, pyrite, rutile ± APS minerals;

Propylitic zone, composed of quartz, albite, calcite, chlorite, pyrite, sericite and epidote.

Chelopech Cu-Au deposit (Bulgaria)

Chelopech Cu-Au Mine: geology model

Brittle deformation in fine-laminated sediment

Matrix-supported monomictic phreatomegmatic breccia

It is interpreted that Chelopech deposit was formed in shallow intrusive setting, related to phreato-magmatic breccias which formed a maar-diatreme and numerous blind breccia-pipe structures.

Chelopech Cu-Au deposit (Bulgaria)

Chelopech Cu-Au Mine: Exploration (as per DPM 2021/03 press release)

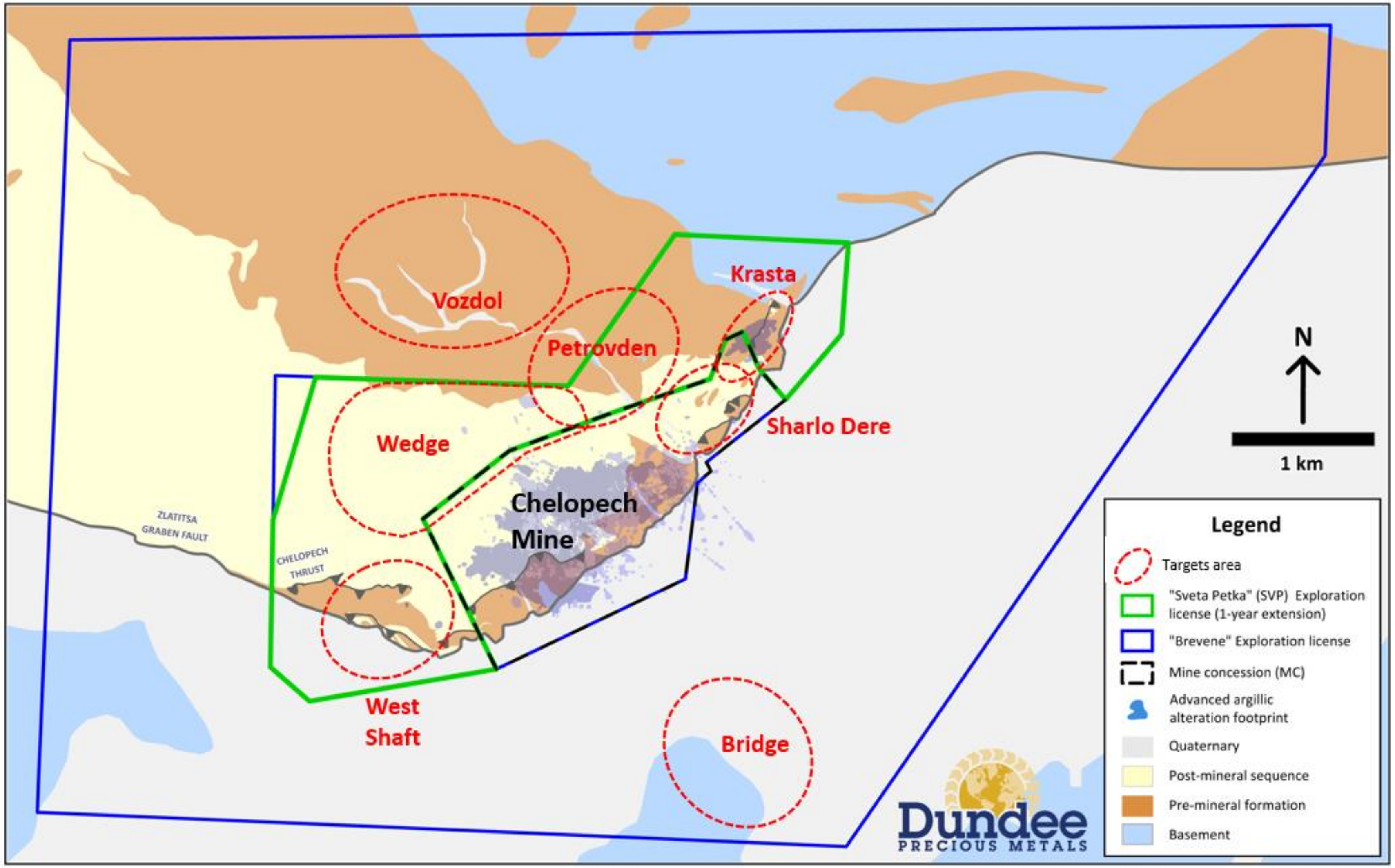

- In January 2021, a Geological Discovery was registered with the Bulgarian Ministry of Energy for the Sveta Petka License.
- In 2021 exploration activities on the Sveta Petka license are focused on infill and extensional drilling required for the technical development of the Wedge, West Shaft, Sharlo Dere and Krasta prospects in conjunction with the Commercial Discovery process.
- On the broader Brevene exploration license scout drilling of priority targets, including the Bridge Target, has commenced. A targeting study to evaluate the Vozdol prospect has been completed and drilling on selected priority targets will commence during the second quarter.

Chelopech Cu-Au deposit (Bulgaria)

Chelopech Cu-Au Mine: geology model, distribution of breccia pipes and ore bodies

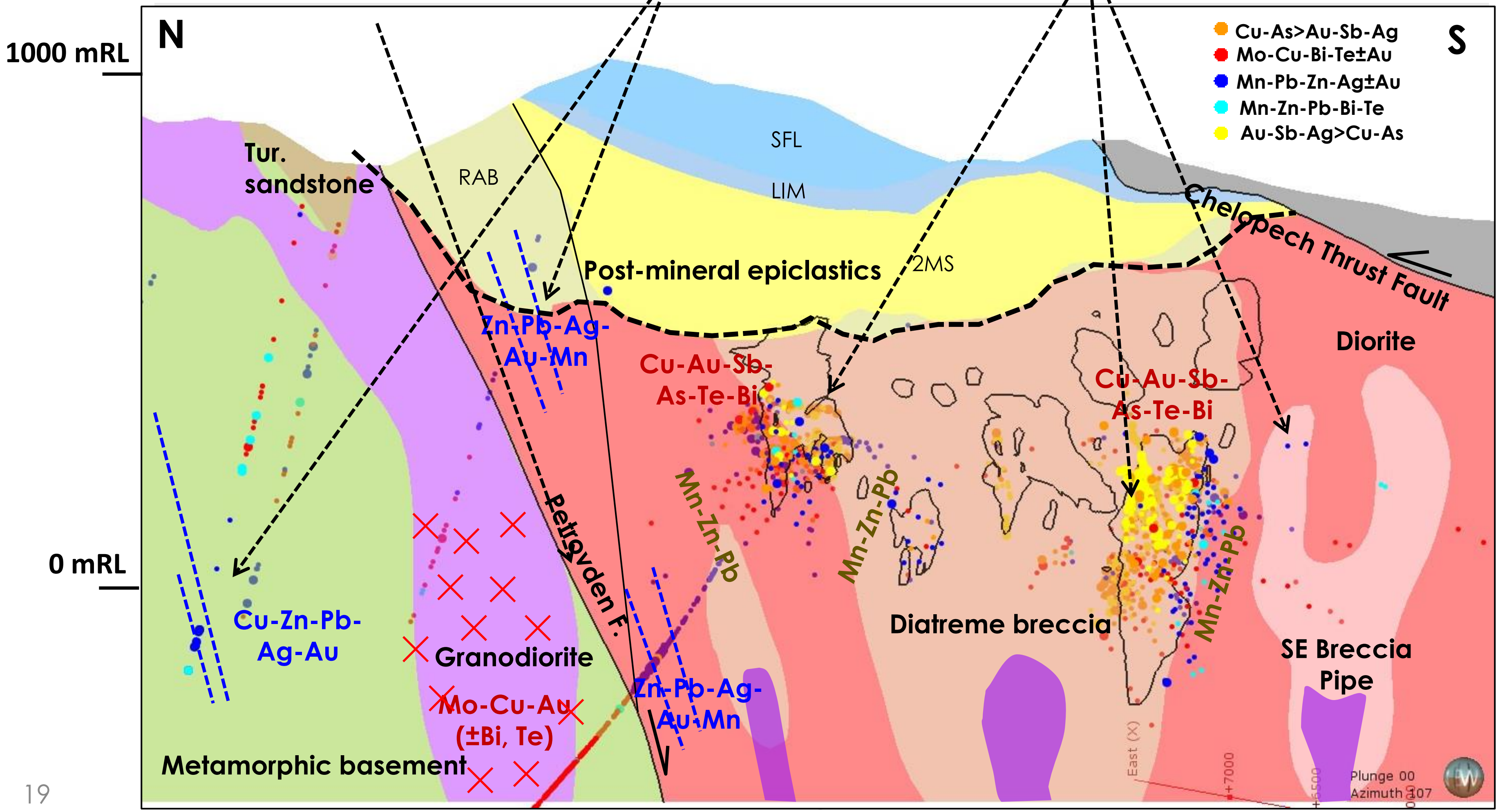

Simplified N-S section (looking to E) through the Vozdol-Petrovden-Chelopech area, showing the distribution patterns of selected ore-related metals (Marton et al 2016)

Zlatica Basin fill

Campanian – Maastrichtian Sedimentary group

Late Turonian Chelopech Mine formation (premineral) 92.2 – 91.3 Ma

Early Turonian Terrigenous Sedimentary group 93.5 Ma

Metamorphic basement

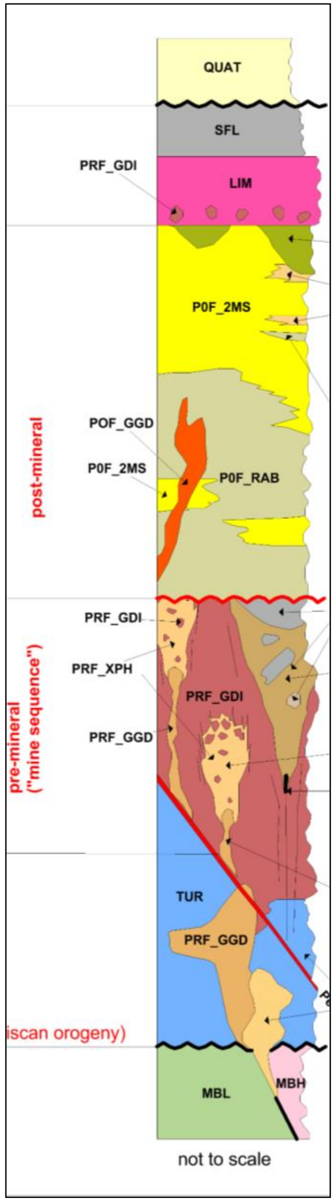

Geochemical vectoring to ore

Alteration & mineralization by core scan

Examples with closer looks of moderately mineralized drill core:

- LWIR SOM Borehole image, with light blue highlighting the sulphide/sulphosalt zones.
- The VN-SWIR map shows that the dominant argillic alteration is represented by dickite, which is locally interfingered by kaolinite and illite zones.

SOM Borehole Image Legend

1 20

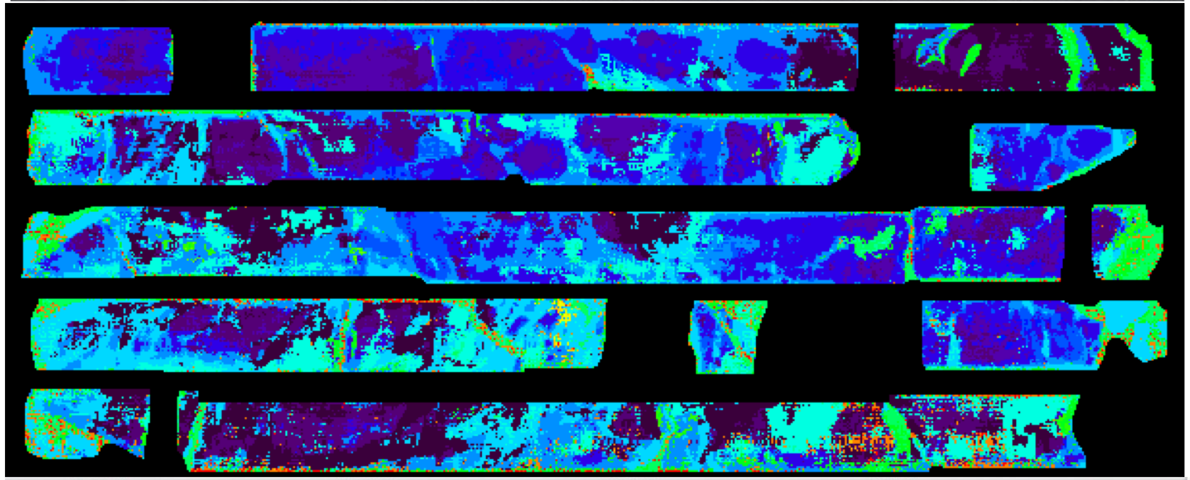

VN-SWIR: Dominant Mineral Map

- Calcite-Illite
- Chlorite
- Dickite
- Fe Carbonate
- Flat Response
- Illite
- Kaolinite-Quartz
- Montmorillonite
- Pyrophyllite
- Uncertain
- Water

Geochemical vectoring to ore

Alteration & mineralization by core scan

Examples with closer looks of weekly mineralized drill core:

- Both SWIR and LWIR maps show the contact between the illite (-quartz) and dickite (-quartz) dominated alteration zones.

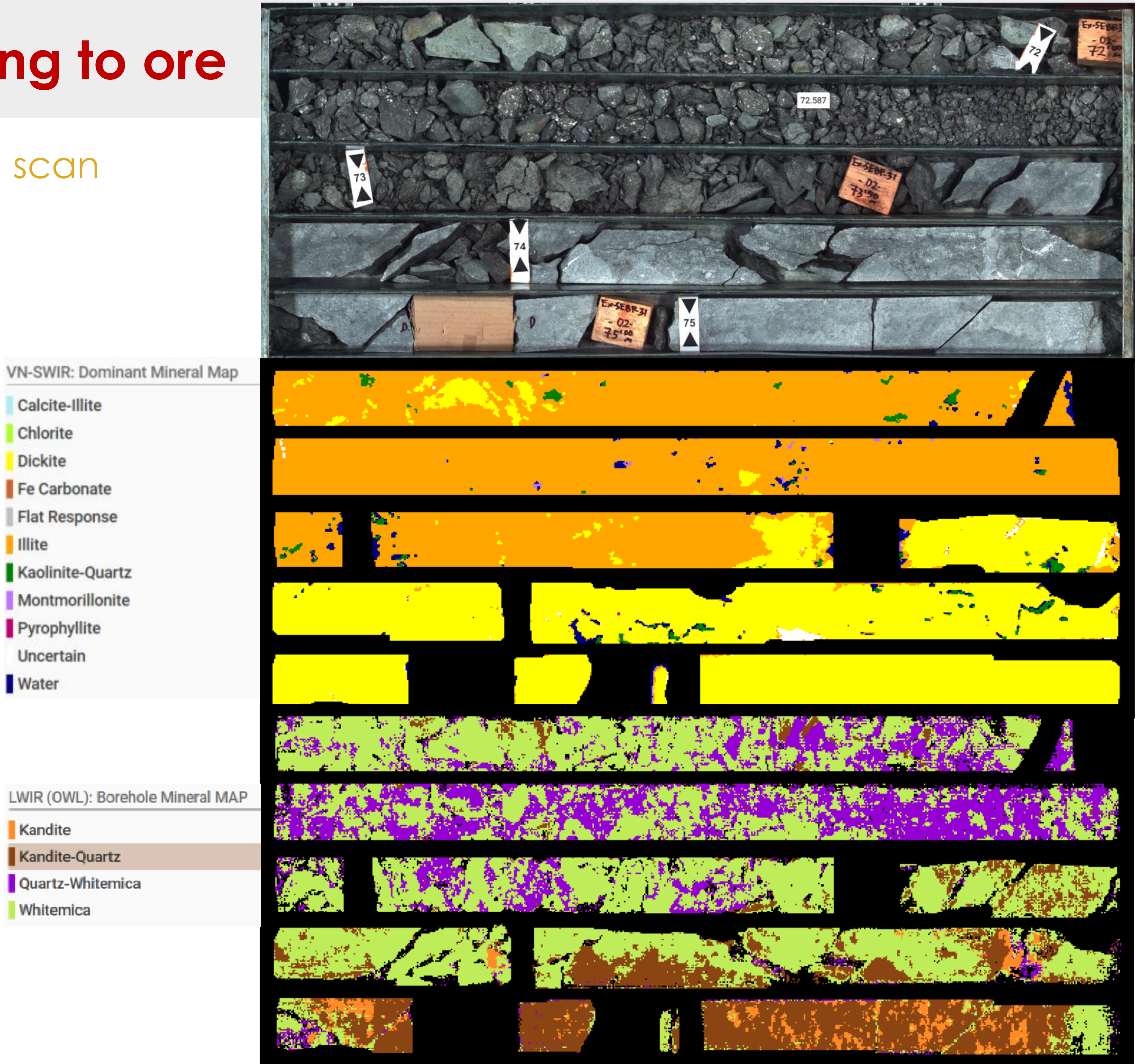

Geochemical vectoring to ore

Alteration & mineralization by core scan

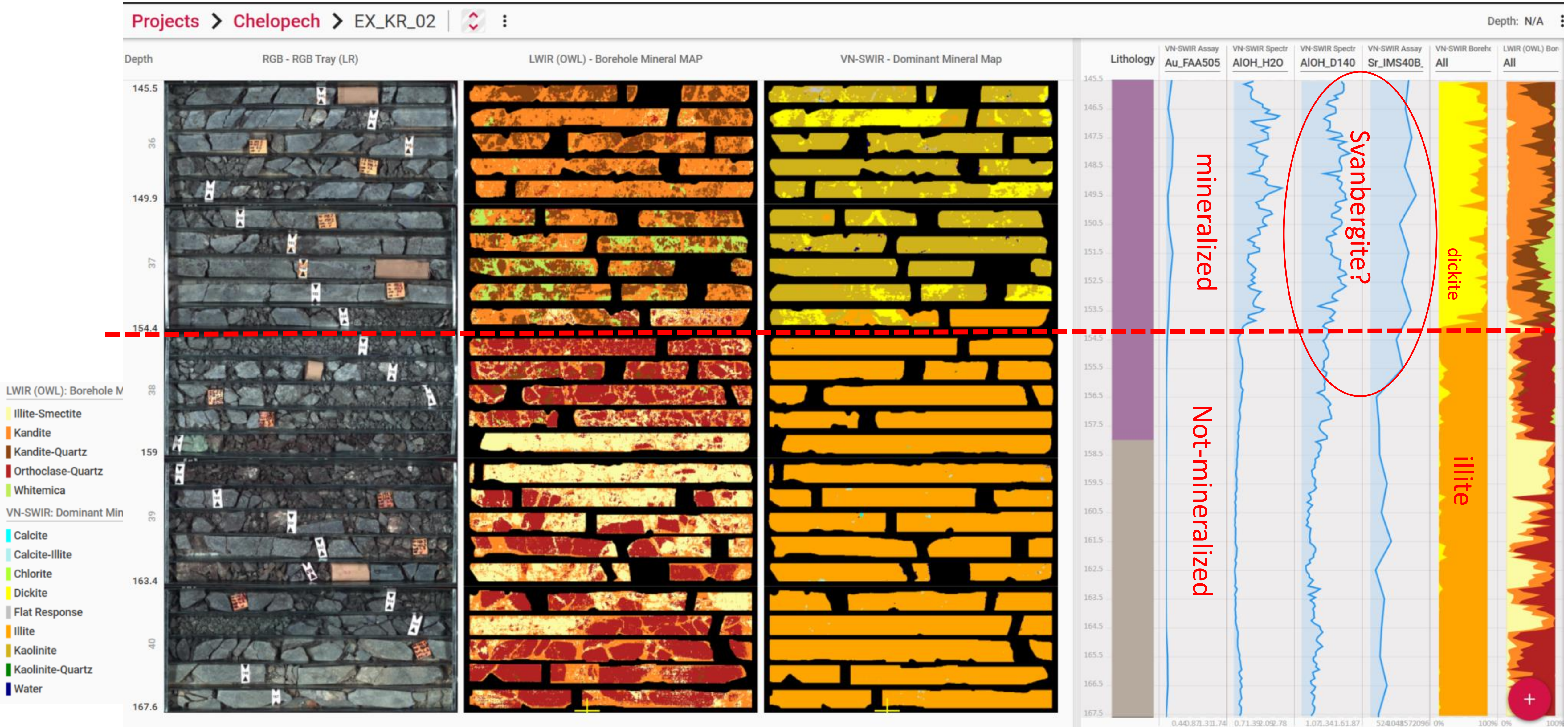

Geochemical vectoring to ore

Alteration boxplot: AI vs. AAAI (4 acid + ICP-MS dataset, calculated Si by summed to 100%)

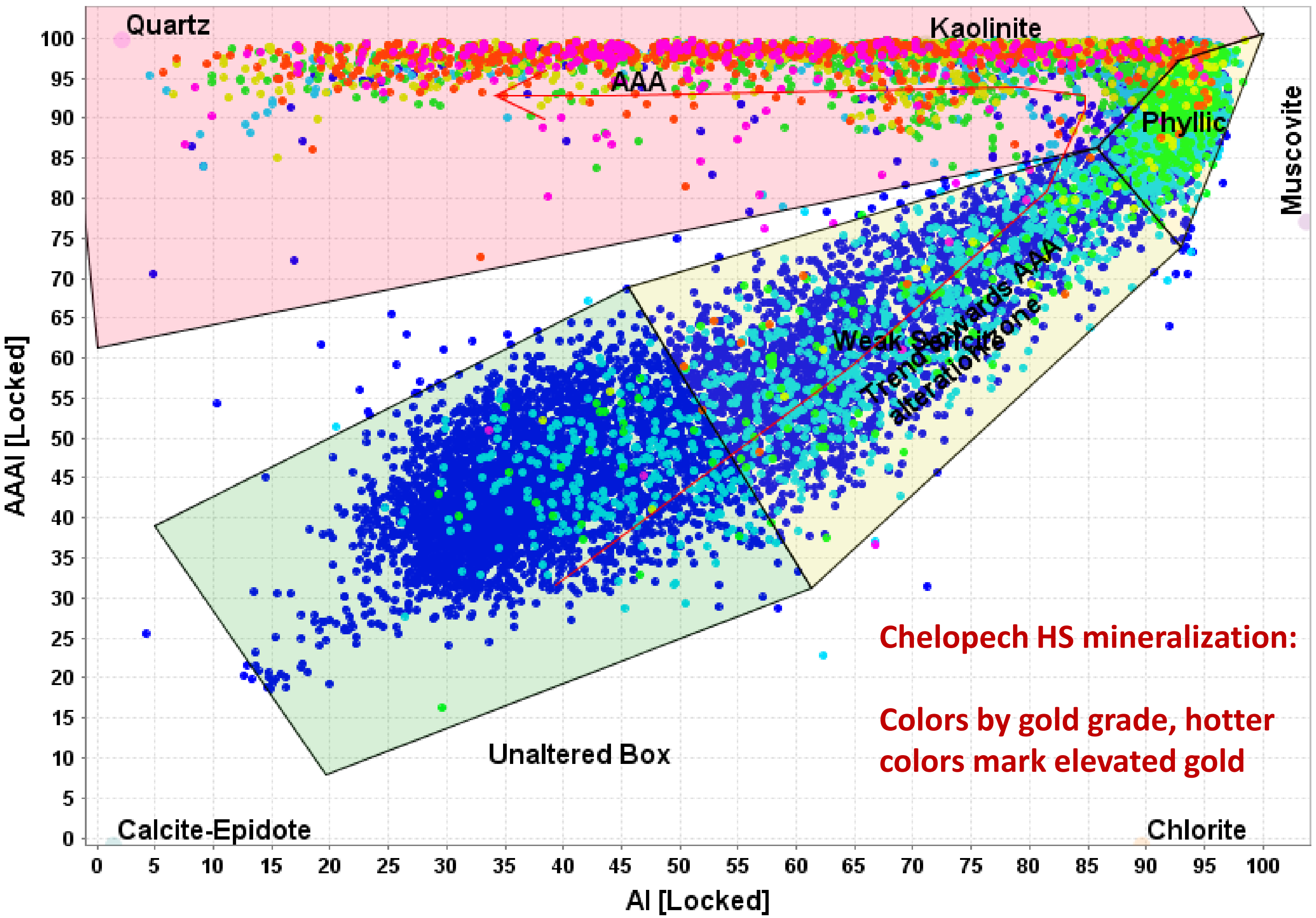

Increase in AAAI represents strong SiO2 enrichment and destruction of chlorite, carbonate and feldspar. These are the mineralogical changes that are also seen in advanced argillic alteration zones in high-sulfidation epithermal systems.

The **Ishikawa Alteration Index** reflects the abundance of chlorite and sericite and depletion of CaO and Na2O associated with feldspar destruction. The arrow on the plot indicates the trend from the unaltered box toward pyrophyllite alteration zones. The box for unaltered samples is defined in the advanced argillic alteration index by the spread of least altered (propylitic) samples as defined in the source paper and in the AI by the least altered box of the Alteration Box Plot by Large et al. (2001).

AAAI = 100 $(SiO_2)/(SiO_2 + 10MgO + 10CaO + 10Na_2O)$

AI = 100*$(MgO+K_2O)/(MgO+Na_2O+CaO+K_2O)$

References:

- Williams, N.C., and Davidson, G.J., 2004, Possible submarine advanced argillic alteration at the Basin Lake prospect, Western Tasmania, Australia: Economic Geology v.99, pp. 987-1002
- Large, R.R. et al., 2001, The alteration box plot: A simple approach to understanding the relationship between alteration mineralogy and lithogeochemistry associated with volcanic-hosted massive sulfide deposits: Economic Geology v.96, pp. 957-972

Geochemical vectoring to ore

Alteration boxplot: AI vs. AAAI (4 acid + ICP-MS dataset, calculated Si by summed to 100%)

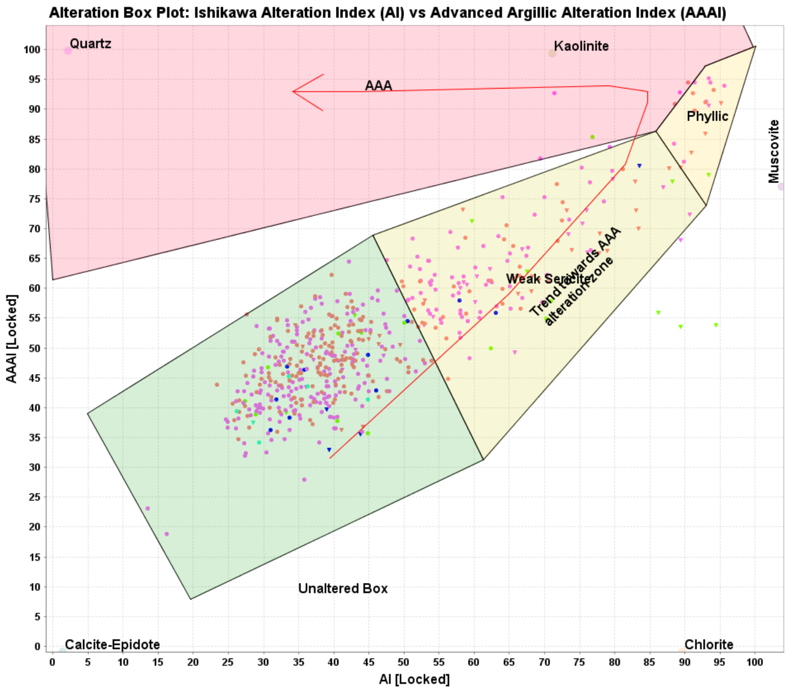

Colour
Min1 sTSAS
- Ankerite
- FeChlorite + FeMgChlorite
- Phengite
- Phengitic Illite + PhengiticIllite
- Prehnite

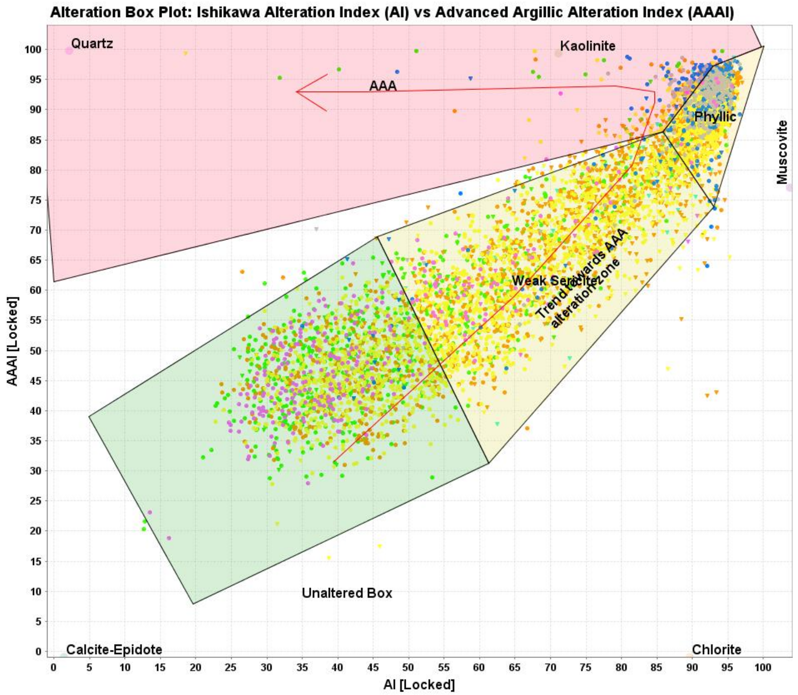

Colour
Min1 sTSAS
- Illite
- Montmorillonite
- Muscovite
- Muscovitic Illite + MuscoviticIllite
- Paragonite
- Paragonitic Illite + ParagoniticIllite
- Phengite

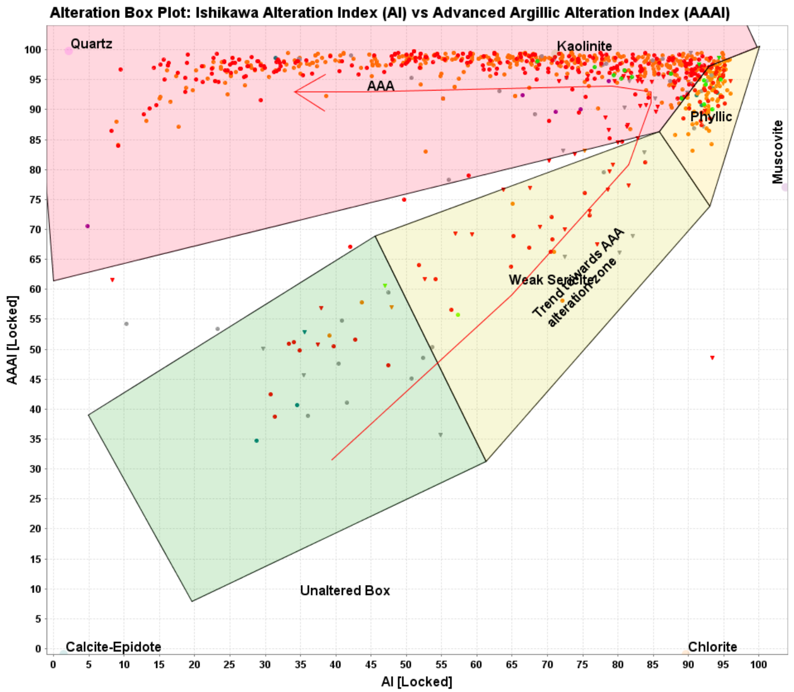

Colour
Min1 sTSAS
- Alunite-K + Alunite-Na + Na_Alunite + K_Alunite
- Diaspore
- Dickite
- Kaolinite PX + Kaolinite-PX
- Kaolinite WX + Kaolinite-WX
- Nontronite
- Pyrophillite + Pyrophyllite

Geochemical vectoring to ore

Alteration zonation using AI vs. AAAI boxplot

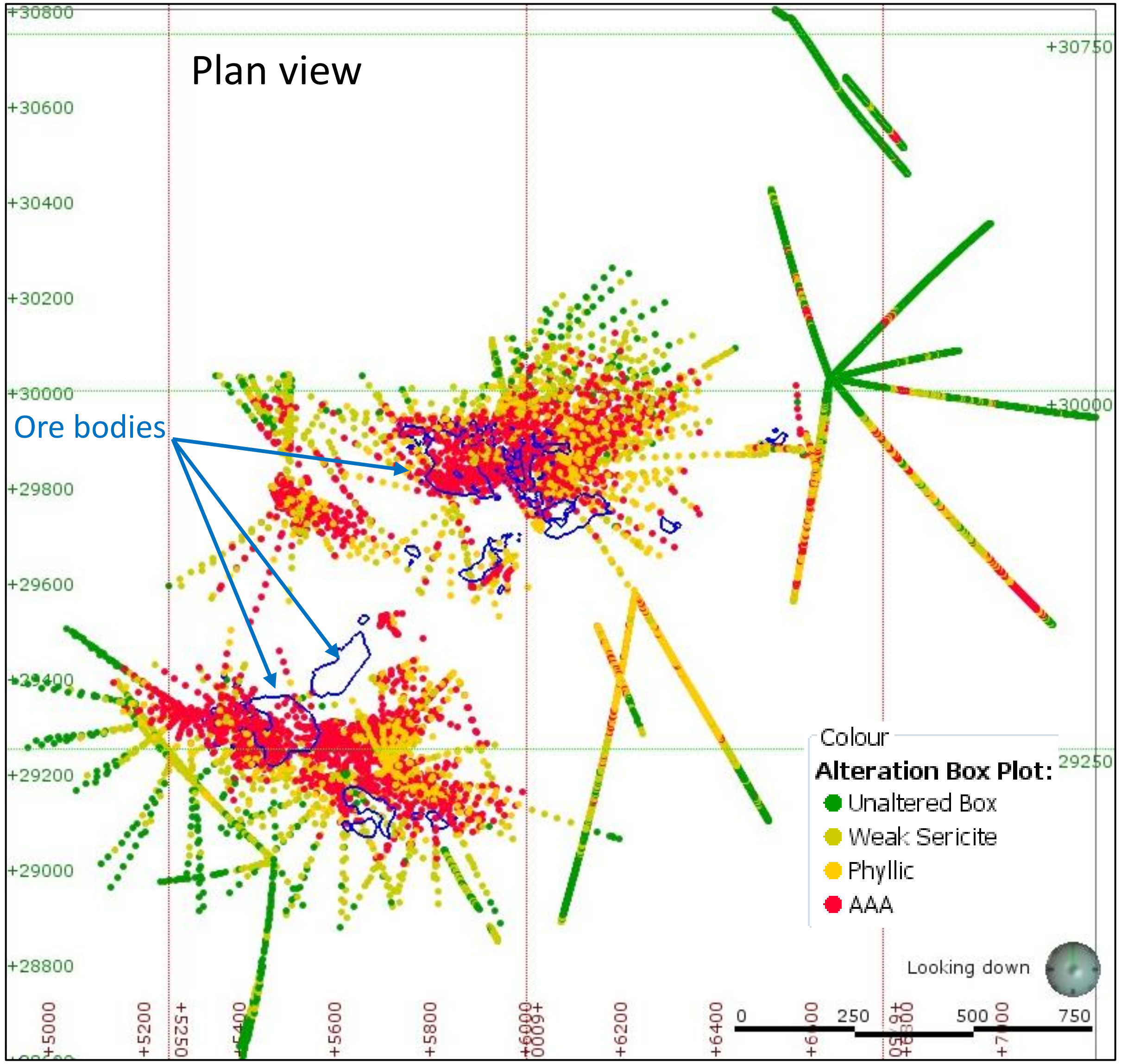

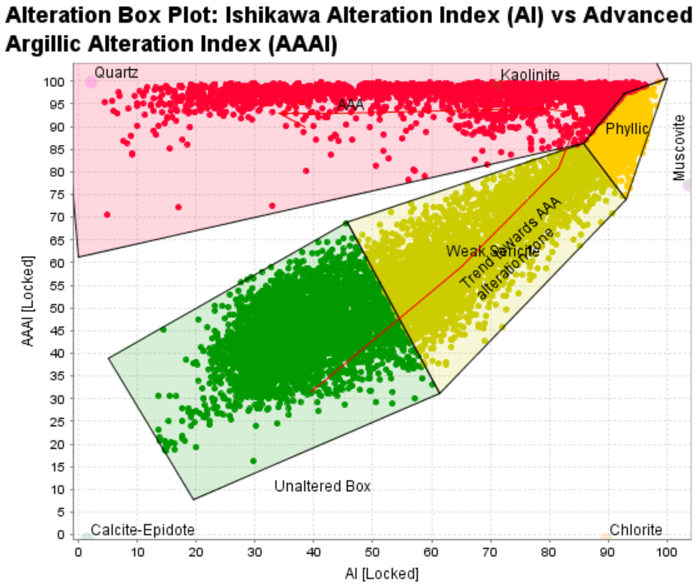

Concerns:

- Si is not measured but calculated without considering LOI content.
- Al is commonly underestimated in APS-rich samples
- Does not provide zonation around ore bodies.
- It works only as broad vector to find the mineralized system.

Geochemical vectoring to ore

Tracing alteration footprint through feldspar destruction and Sr, Ca, K and Sc zonation

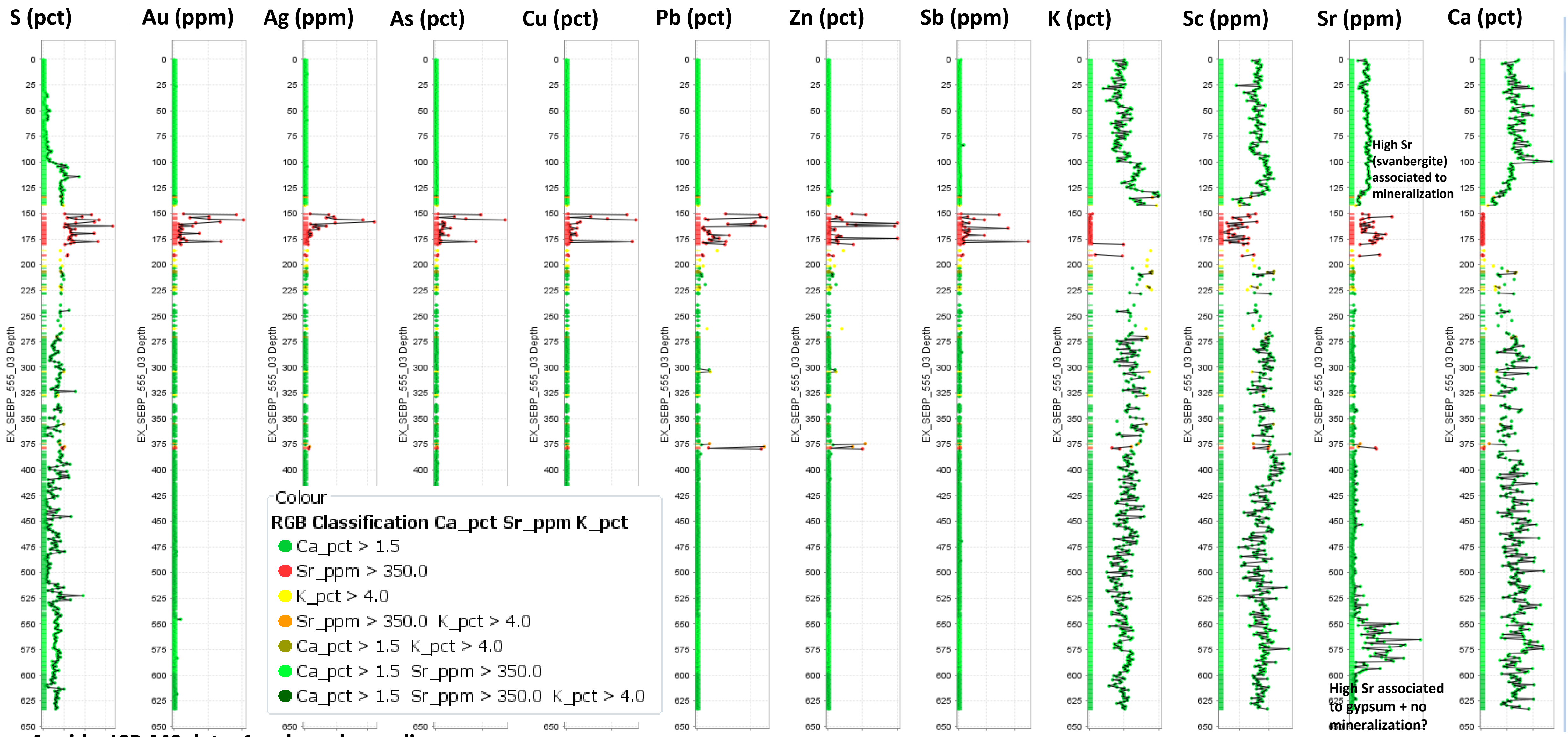

4 acid + ICP-MS data, 1 m-based sampling

Geochemical vectoring to ore

Tracing alteration footprint through feldspar destruction and Sr, Ca, K and Sc zonation

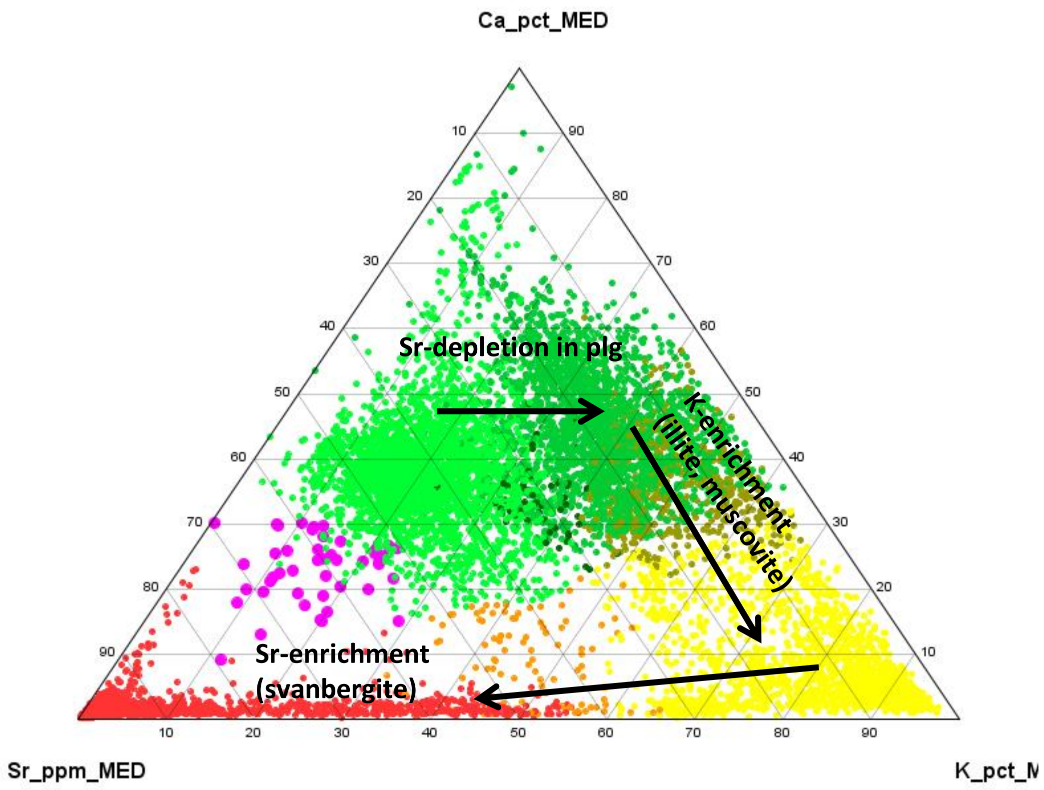

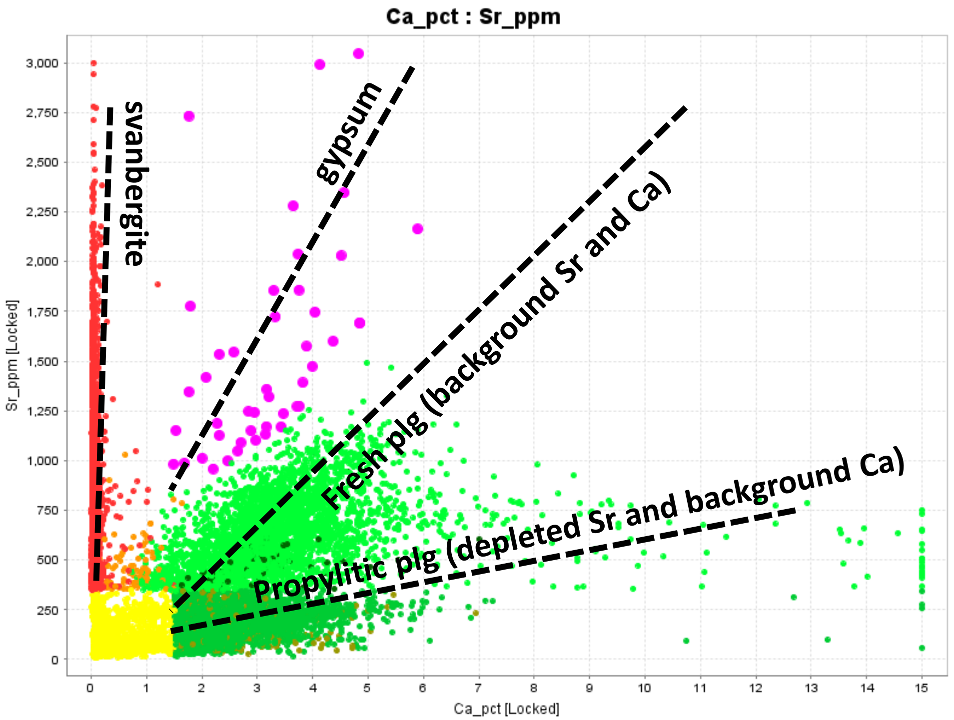

4 acid + ICP-MS data, 1 m-based sampling

Geochemical vectoring to ore

Tracing alteration footprint through feldspar destruction and Sr, Ca, K and Sc zonation

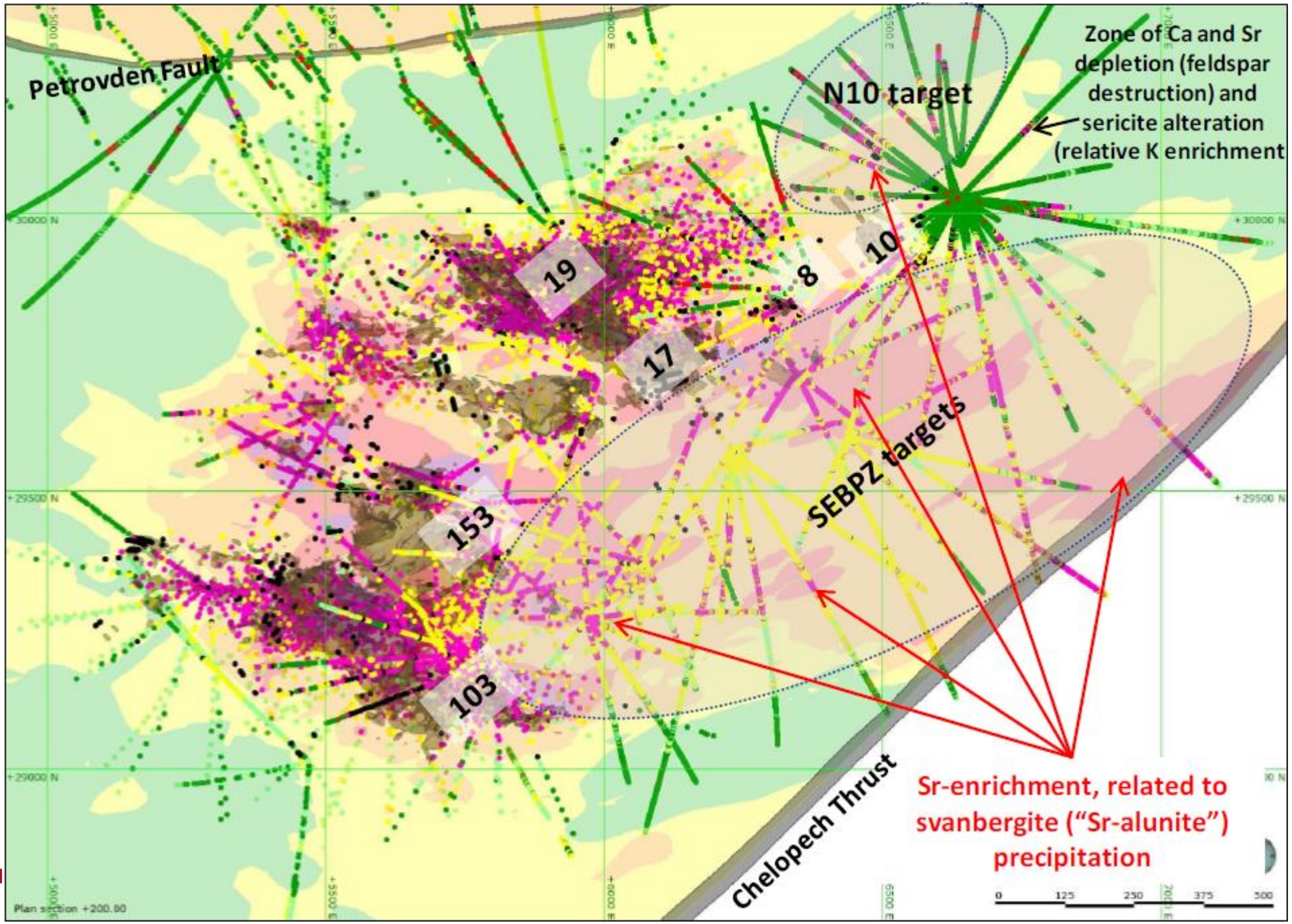

Lithophile element provide a primary vector to mineralization within this alteration footprint. Proxy indicators for different alteration zones are the following:

- Ca-depletion shows destruction of feldspar, therefore the general envelope of alteration footprint;
- K-enrichment occurs within illite-rich zone, in outer margin of mineralized zones;
- Sr-enrichment occurs in central core of AAA zones (hot fluids vents, ASP minerals precipitation) forming the core of economic mineralization.

Using the relative distribution of the Ca, K and Sr an alteration classification was created, which enabled tracing within the alteration footprint.

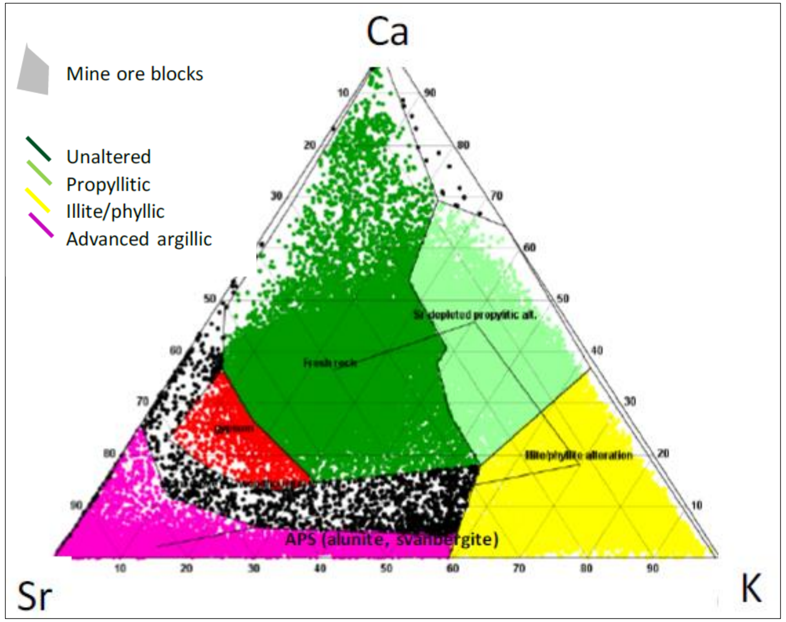

Geochemical vectoring to ore

Tracing alteration footprint through feldspar destruction and Sr, Ca, K and Sc zonation

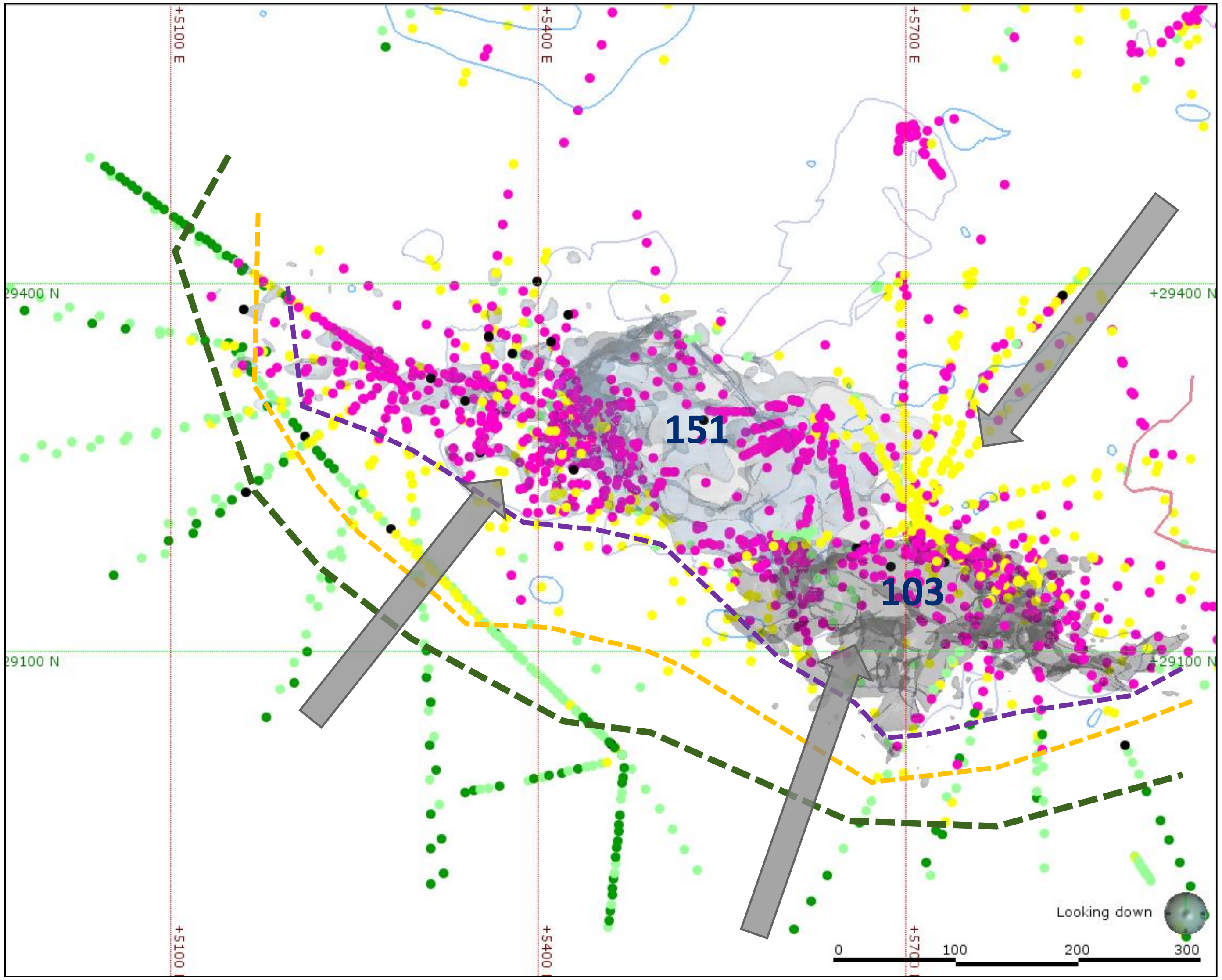

Vectoring footprint:

- Major western ore bodies express well the Sr-K-Ca alteration zonation, with vector from fresh rock -> Sr-depleted propylitic alteration -> illite/muscovite alteration -> AAA alteration (with svanbergite).
- Vectored footprint around ore bodies extend to 150-200 meters

gypsum
Fresh rock
Sr-depleted propylitic alt.
Illite/phyllite alteration
svanbergite (+/- woodhousite) in AAA

Geochemical vectoring to ore

Tracing alteration footprint through feldspar destruction and Sr, Ca, K and Sc zonation

Optimal drill spacing in the footprint:

- DH at 200m spacing could potentially miss smaller (~0.5 Mt) northern ore body, but would intersect the illite/phyllic halo (K-enrichment);
- Following-up vectoring and drillhole infill could potentially intersect the orebody;
- Observe also strong AAA zone with new potential.

gypsum
Fresh rock
Sr-depleted propylitic alt.
Illite/phyllite alteration
svanbergite (+/- woodhousite) in AAA

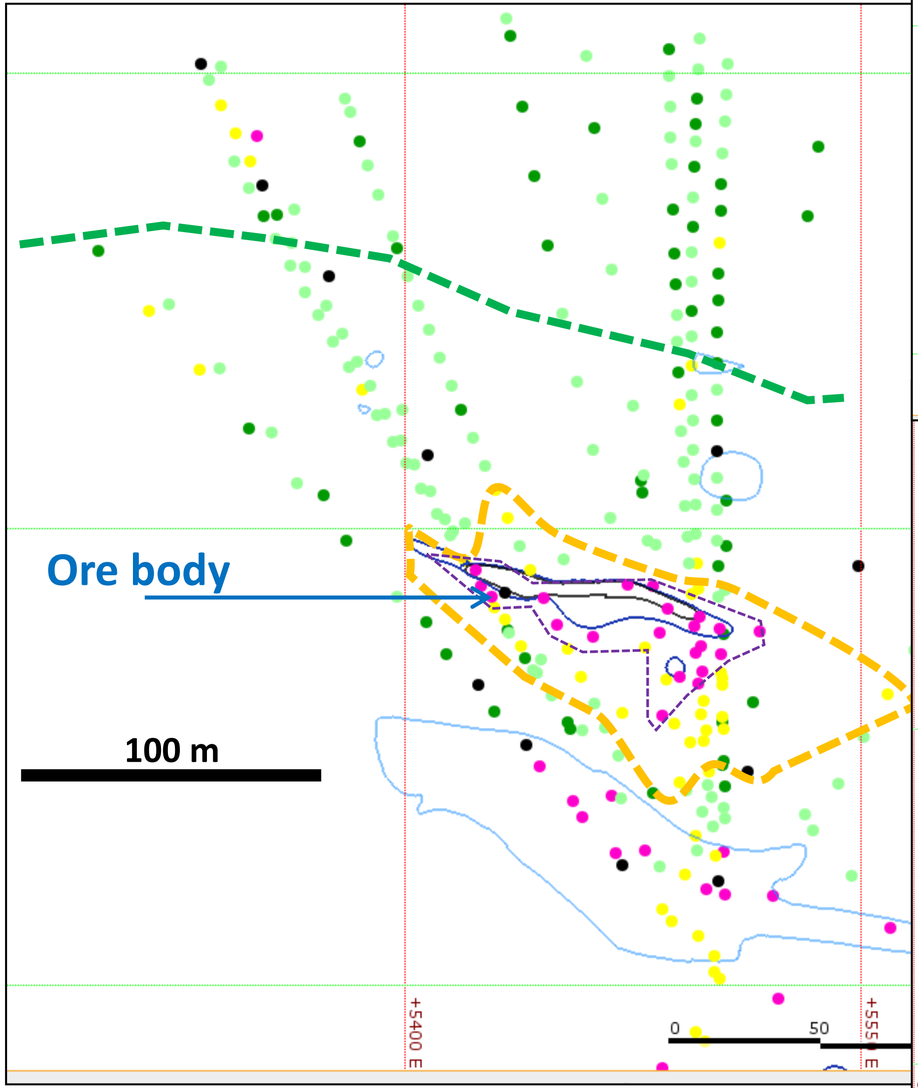

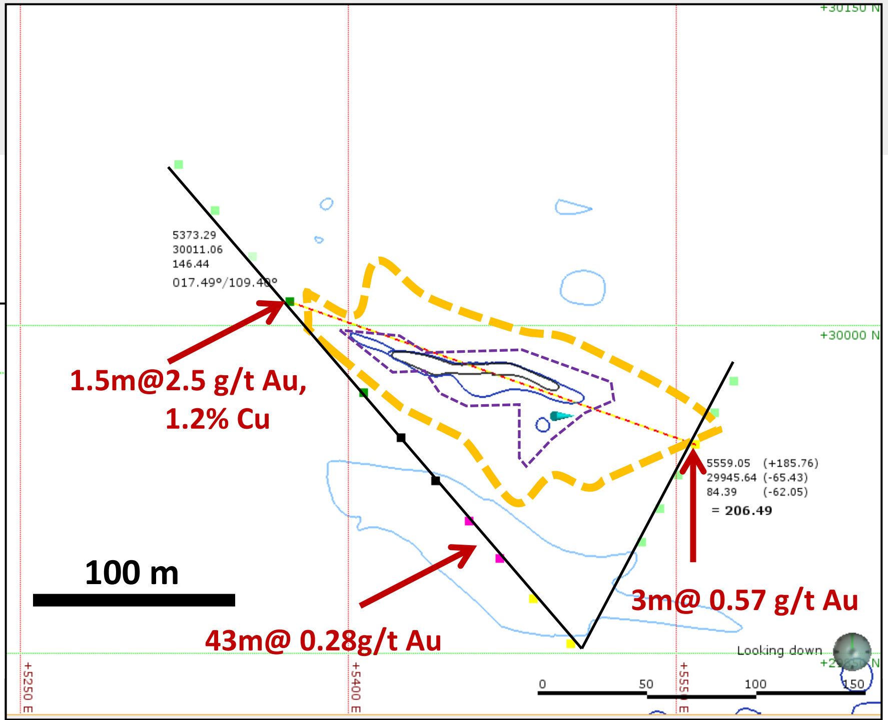

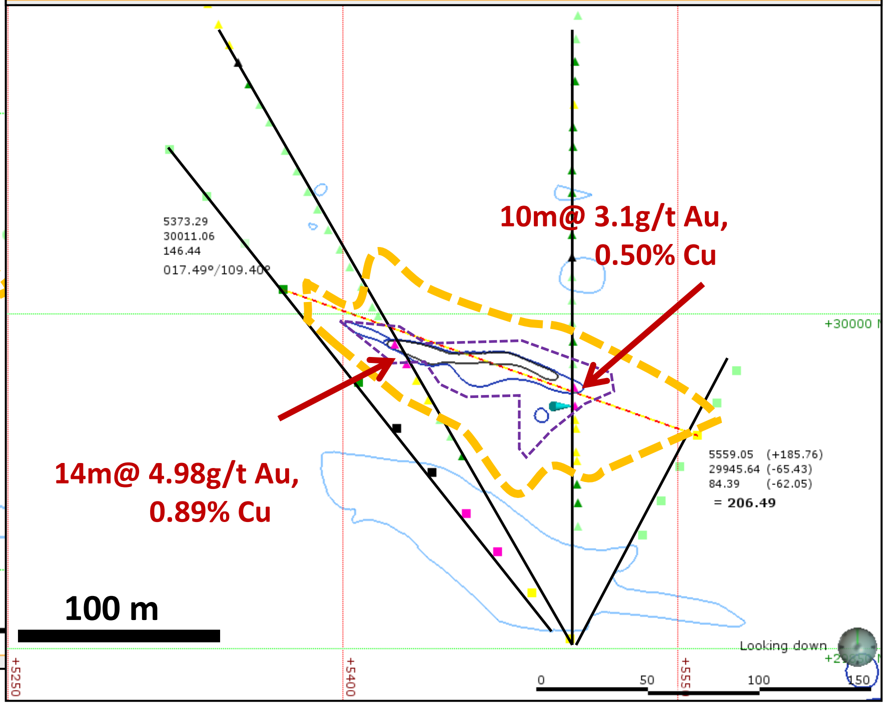

Geochemical vectoring to ore

Au, Cu and other associated metals vs. alteration zones (probability plots)

2 and 4 acid + ICP-MS data

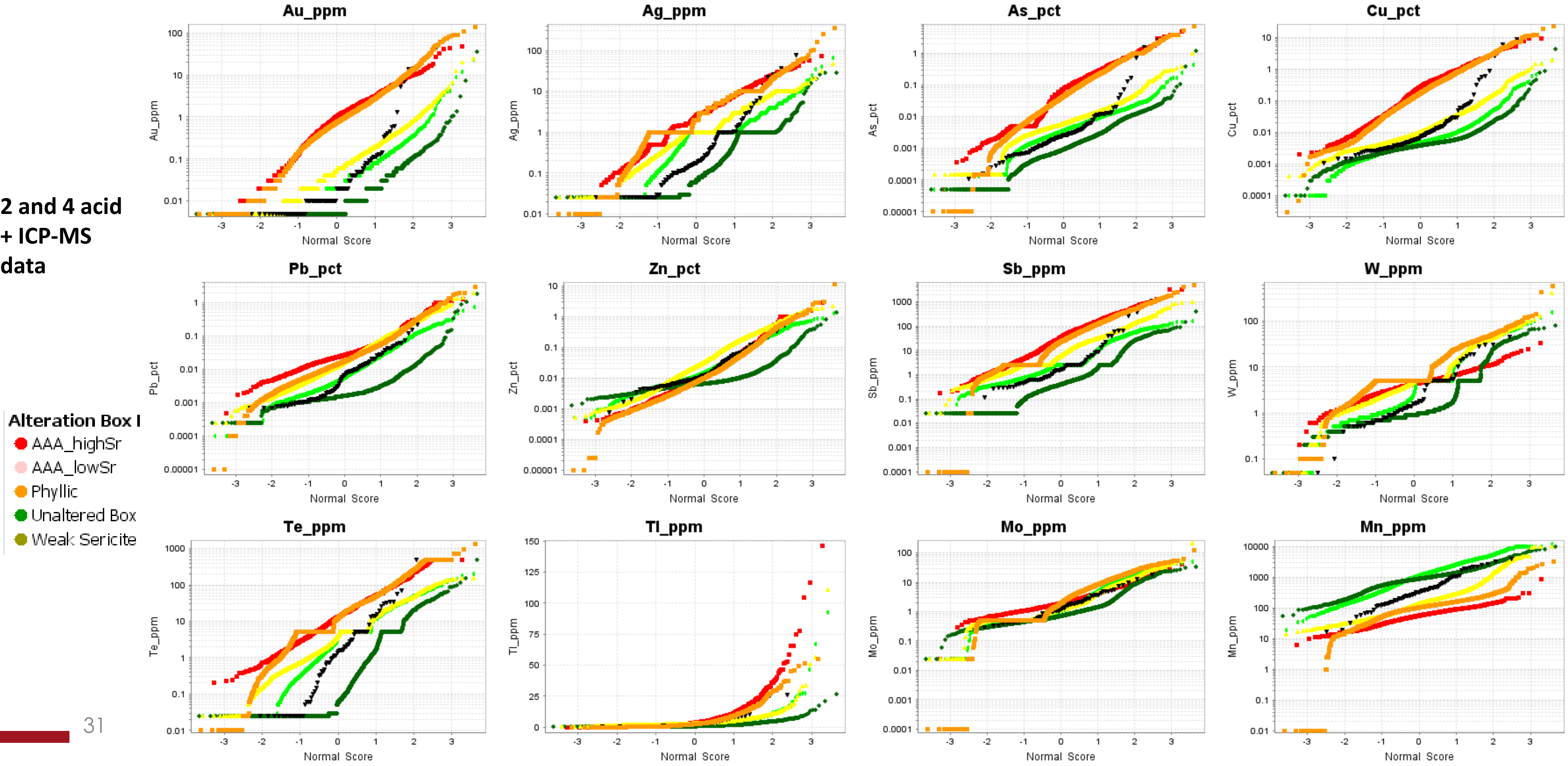

Geochemical vectoring to ore

Au, Ag, As, Sb, Bi, Cu, Mo, Mn, Te, Pb, Zn association : Principal Component Analysis

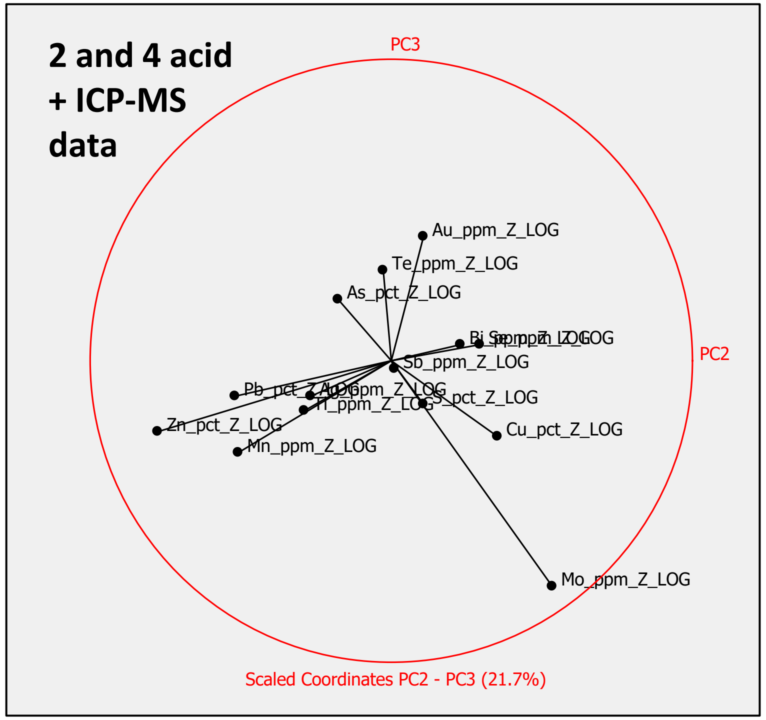

Eigenvectors	PC1	PC2	PC3	PC4	PC5	PC6	PC7	PC8	PC9	PC10	PC11	PC12	PC13	PC14
Au_ppm_Z_LOG	0.2094	0.07978	0.3818	0.6471	0.08186	0.4959	0.2328	0.151	0.201	0.06991	0.02971	0.02815	0.03778	0.08469
Cu_pct_Z_LOG	0.2919	0.2581	-0.2359	0.2247	-0.133	-0.1563	0.09215	-0.2313	-0.0709	0.1836	0.3526	-0.3283	0.2789	-0.5378
Ag_ppm_Z_LOG	0.2928	-0.1965	-0.1084	0.1257	-0.2571	0.117	-0.5583	0.5413	-0.2416	0.06373	-0.09039	-0.01709	-0.1975	-0.2318
As_pct_Z_LOG	0.2846	-0.1289	0.189	0.1383	0.3361	-0.6203	0.08653	0.3163	0.149	-0.335	-0.197	-0.1913	0.1796	-0.00996
Bi_ppm_Z_LOG	0.326	0.1664	0.05093	-0.01776	-0.1426	-0.1053	-0.09695	-0.05552	-0.1296	-0.2333	0.5497	-0.1973	-0.2927	0.5667
Mn_ppm_Z_LOG	-0.1969	-0.37	-0.2852	0.4667	0.2952	-0.04968	-0.4766	-0.3642	0.1093	0.03903	0.06305	-0.1016	0.08861	0.2003
Mo_ppm_Z_LOG	0.08448	0.3888	-0.6971	0.2204	0.02713	0.05731	0.149	0.1309	-0.00299	-0.3333	-0.2233	0.287	0.003365	0.143
Pb_pct_Z_LOG	0.2703	-0.3781	-0.1083	-0.1342	-0.3408	0.07997	0.1053	0.03741	-0.02403	0.07999	0.02237	0.1552	0.6924	0.3292
Sb_ppm_Z_LOG	0.3252	0.00928	-0.02576	0.1125	0.07866	-0.3629	0.1237	-0.1315	-0.1133	0.6622	-0.1732	0.3532	-0.2719	0.174
Te_ppm_Z_LOG	0.3156	-0.01795	0.2793	0.006622	0.01158	0.02279	-0.2175	-0.4579	-0.1553	-0.4252	-0.02471	0.5373	0.02242	-0.264
Zn_pct_Z_LOG	0.1566	-0.5633	-0.2182	0.03553	-0.2663	0.03725	0.4031	-0.1613	0.2694	-0.1856	-0.02608	-0.102	-0.4495	-0.1681
S_pct_Z_LOG	0.2953	0.07731	-0.1327	-0.3542	0.2837	0.1454	-0.229	0.09712	0.7045	0.1323	0.2333	0.1597	-0.00568	-0.08105
Se_ppm_Z_LOG	0.3106	0.2128	0.04791	-0.1386	-0.1199	0.177	-0.1825	-0.3375	0.112	0.01529	-0.6194	-0.4726	-0.00351	0.155
Tl_ppm_Z_LOG	0.2557	-0.2099	-0.1526	-0.229	0.6325	0.349	0.1936	0.00503	-0.4758	0.01096	0.04343	-0.1617	-0.01039	-0.02932
Eigenvalues	7.428	1.887	1.152	0.8272	0.5897	0.4335	0.3443	0.2817	0.2437	0.2083	0.1979	0.1424	0.1345	0.1305
Percent	53.05	13.48	8.228	5.908	4.212	3.097	2.459	2.012	1.74	1.488	1.413	1.017	0.9611	0.9324
Cumulative %	53.05	66.53	74.76	80.67	84.88	87.98	90.44	92.45	94.19	95.68	97.09	98.11	99.07	100

- Quick PCA highlights at least 3 major ore types:
  - Porphyry Cu-Mo-Bi
  - HS epithermal Au-As-Sb-Te
  - Distal Ag- Pb-Zn-Mn

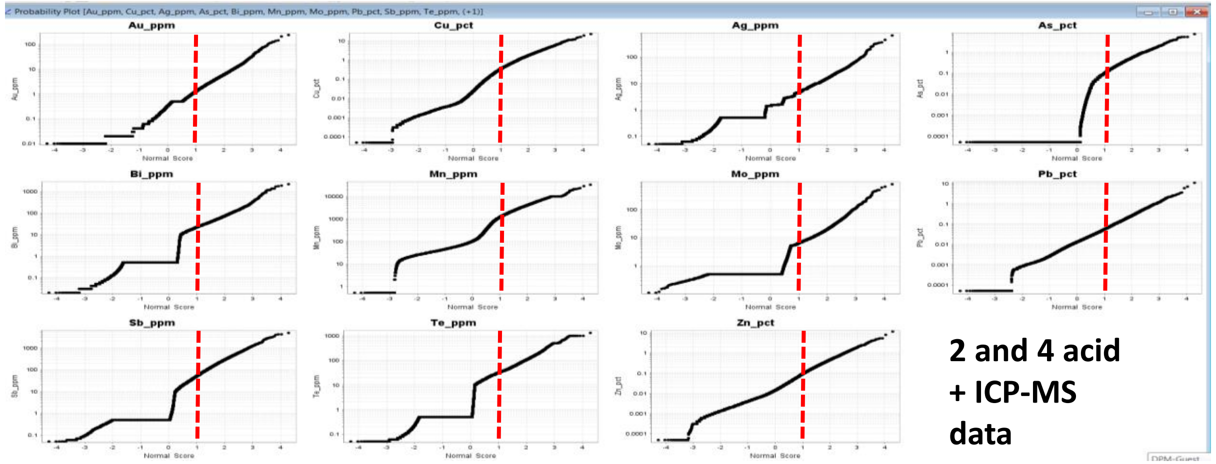

Note that probability plots suggest for normal scores >1 all elements show accepted distribution, while for <1 normal scores data distribution for certain elements (Ag, Mo, Bi, Mn) is problematic due to various analytical procedures and detection limits. For next steps we only use >1 z-scores assays.

Geochemical vectoring to ore

Au, Ag, As, Sb, Bi, Cu, Mo, Mn, Te, Pb, Zn association : WTSR and RGB zonation

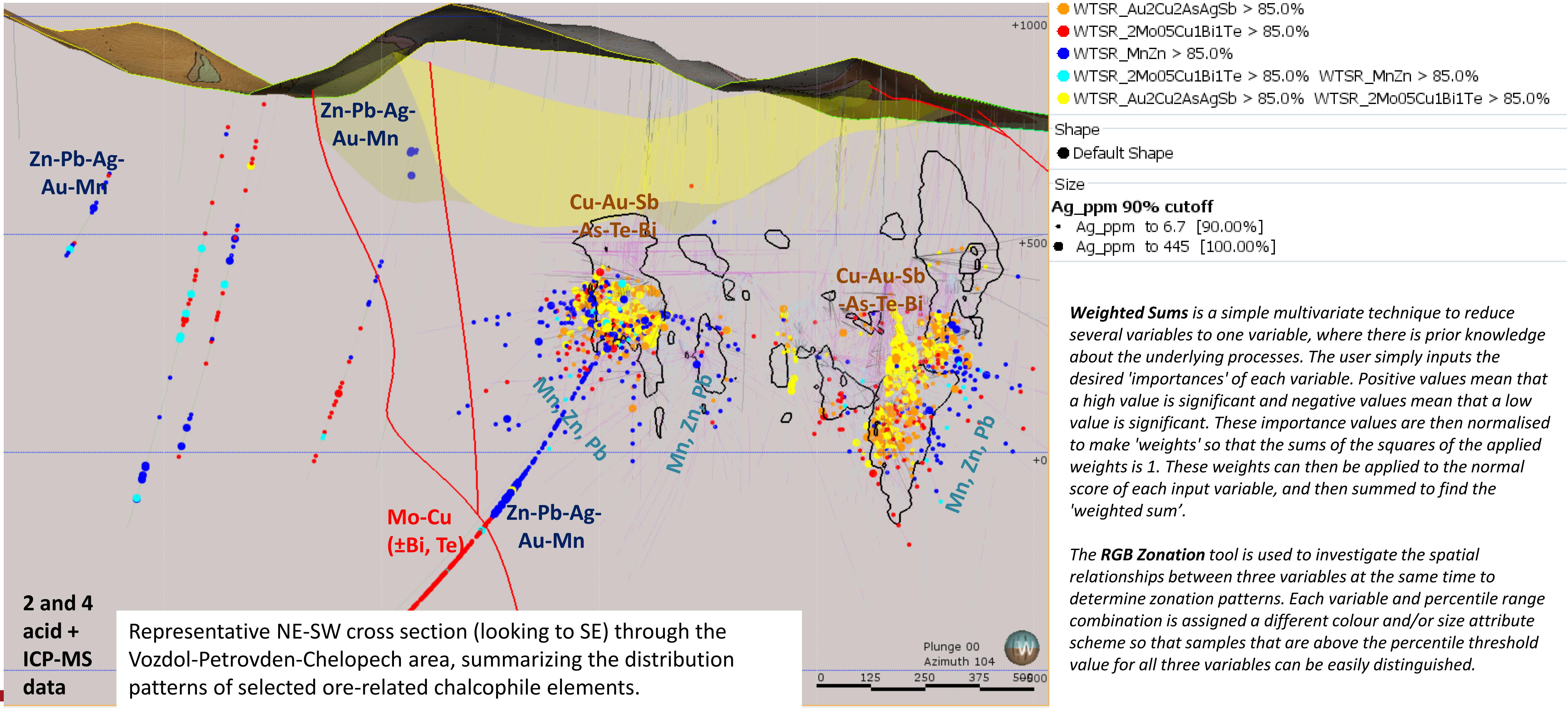

2 and 4 acid + ICP-MS data

Representative NE-SW cross section (looking to SE) through the Vozdol-Petrovden-Chelopech area, summarizing the distribution patterns of selected ore-related chalcophile elements.

Weighted Sums *is a simple multivariate technique to reduce several variables to one variable, where there is prior knowledge about the underlying processes. The user simply inputs the desired 'importances' of each variable. Positive values mean that a high value is significant and negative values mean that a low value is significant. These importance values are then normalised to make 'weights' so that the sums of the squares of the applied weights is 1. These weights can then be applied to the normal score of each input variable, and then summed to find the 'weighted sum'.*

The ***RGB Zonation*** *tool is used to investigate the spatial relationships between three variables at the same time to determine zonation patterns. Each variable and percentile range combination is assigned a different colour and/or size attribute scheme so that samples that are above the percentile threshold value for all three variables can be easily distinguished.*

Geochemical vectoring to ore

Metal zonation HS ore bodies: WTSR and RGB zonation

Looking to East

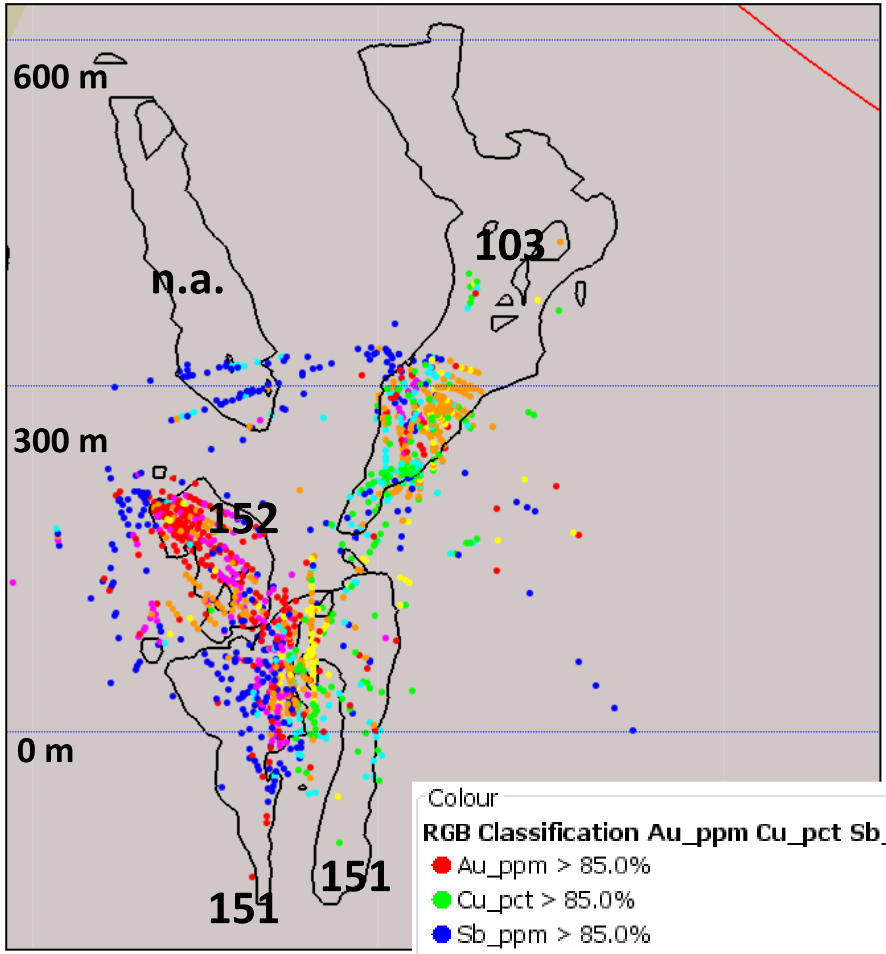

Distribution of chalcophile elements suggest that the HS ore bodies represent single system, but with zoned metal pattern (implications for vectoring and metallurgy):

- Outer Pb, Zn, Tl, Ag +/- Au (Mn)
- Inner Cu, Au, As, Ag, Te
- Core Au, Sb, Bi, Te
- Deep Au, W, Sb, Bi

2 and 4 acid + ICP-MS data

Looking to East

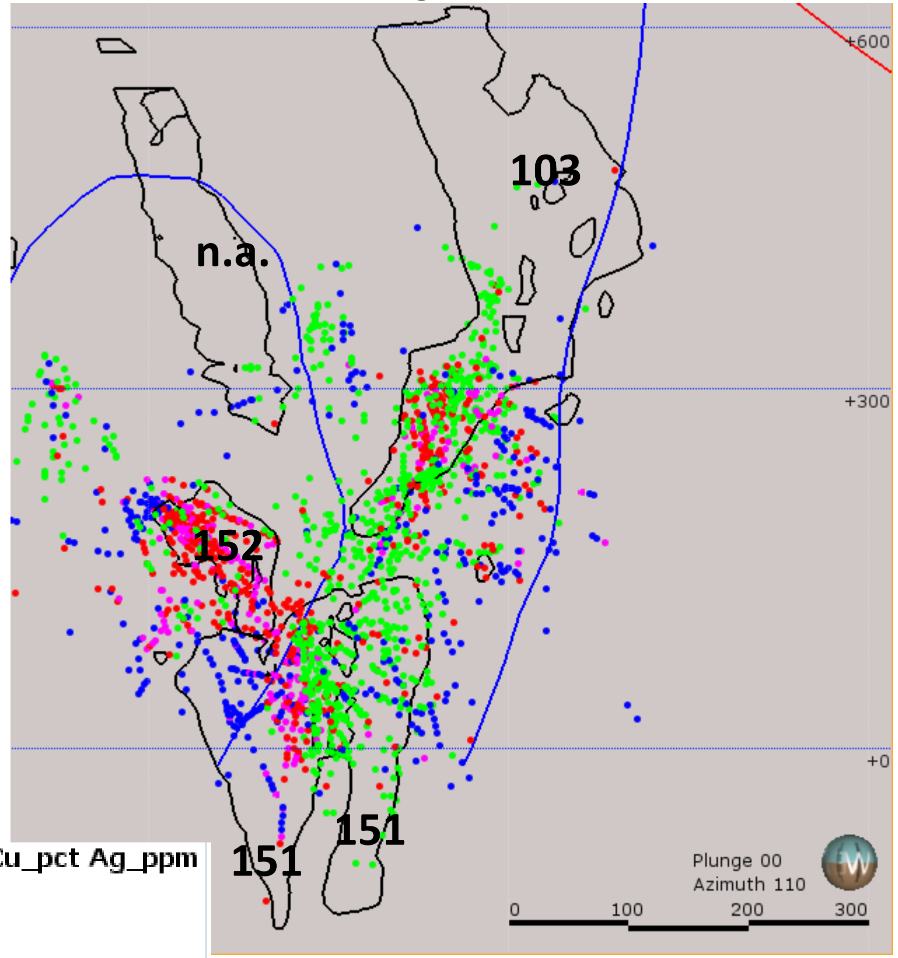

Geochemical vectoring to ore

Relation of HTA footprint size, metal zonation, potential ore body size and guidance for drill spacing

- The alteration and metal zonation model used for the Chelopech HS system shows a relationship between the size of the alteration footprint, the size of the orebodies as well as their metal zonation from outer to inner (core/economic) parts.
- Useful guide to determine the prospectivity, targeting potential and drilling spacing. By enlarging the size of the target by means of measuring alteration and the metal zonation, the drill spacing can be enlarged to the extent that many undercover areas can be prospected with a reasonable degree of reliability.

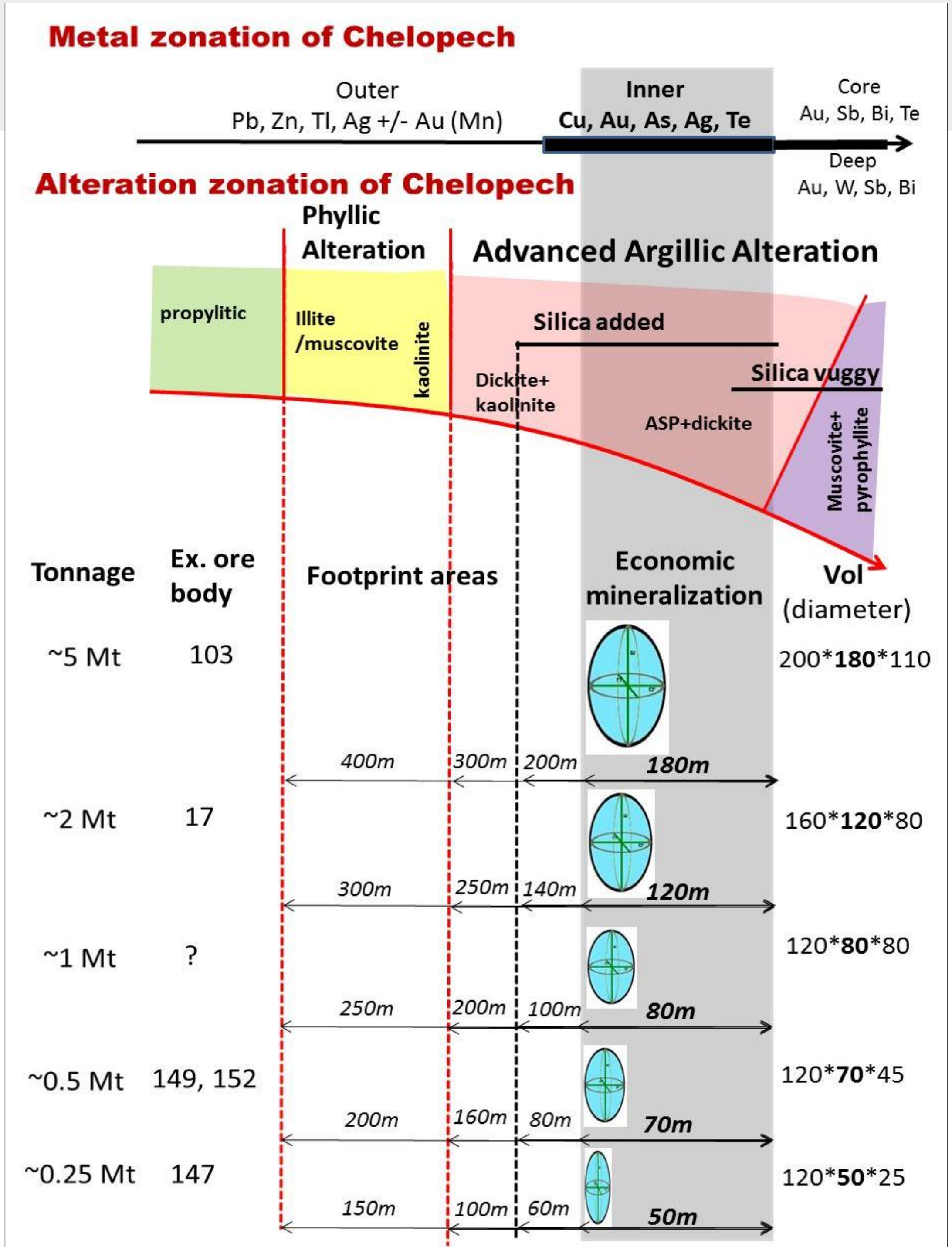

Long-term and creative professional collaboration environment and teamwork with Dundee Precious Metals and agreement to share exploration geochemical information for academic purposes is greatly appreciated.

Thank you for your attention!

DIM ESEE 2: IMPLEMENTING INNOVATIONS

Innovation in Exploration

Dubrovnik, Croatia / hybrid mode - October 20th – 22nd, 2021